Consumers Energy

A CMS Energy Company

Palisades Nuclear Plant
27780 Blue Star Memorial Highway
Covert, MI 49043

Tel: 616 764 2276
Fax: 616 764 3265

Nathan L. Haskell
Director, Licensing and
Performance Assessment

July 6, 2000

U.S. Nuclear Regulatory Commission
ATTN: Document Control Desk
Washington, DC 20555-0001

DOCKET 50-255 - LICENSE DPR-20 - PALISADES PLANT
Reply to Request for Additional Information Regarding Reactor Pressure Vessel Neutron Fluence Evaluation (TAC No. MA8250)

In a letter dated February 21, 2000, Consumers Energy Company submitted revised neutron fluence estimates for the Palisades reactor pressure vessel, and requested NRC approval of a new date by which the reactor vessel is estimated to reach the pressurized thermal shock screening criteria. By letter dated May 25, 2000, NRC requested additional information regarding that submittal. This letter responds to that request.

The letter of February 21 submitted a Westinghouse report (WCAP 15353) which contained an extensive discussion of the methodology used to calculate the Palisades reactor pressure vessel fluence. In this report the predicted fluence was based solely on the results of the absolute transport calculations. In addition, to permit comparison with previous analyses, WCAP 15353 also contained considerable discussion pertaining to adjustment of measured surveillance data. The Least Squared Adjustment (LSA) approach was not used in the February 21, 2000 submittal to derive projected fluence for Palisades. However, this may not have been articulated clearly enough since several of the questions in the Request for Additional Information (RAI) pertain to this LSA methodology. Therefore, to avoid further confusion, the RAI responses are provided in two groups. Attachment 1 provides responses to those questions that relate directly to the methodology used to predict the Palisades fluence values. Responses to the remaining RAI questions that pertain to the LSA methodology are provided in Attachment 2.

A001

SUMMARY OF COMMITMENTS

This letter contains no new commitments and no revisions to existing commitments.

Nathan L. Haskell
Director, Licensing and Performance Assessment

CC Administrator, Region III, USNRC
Project Manager, NRR, USNRC
NRC Resident Inspector - Palisades

Attachments

ATTACHMENT 1

CONSUMERS ENERGY COMPANY
PALISADES PLANT
DOCKET 50-255

July 6, 2000

Reply to Request for Additional Information Regarding Reactor Pressure Vessel Neutron Fluence Evaluation

47 Pages

Reply to Request for Additional Information Regarding Reactor Pressure Vessel Neutron Fluence Evaluation

NRC Question 1

One of the updates in WCAP-15353 uses CASMO-4 for the calculation of the neutron source. However, the CASMO-4 qualifications for this particular application are not discussed. In this instance, it is the prediction of the flux slope at the outer fuel assemblies that matters. How was CASMO-4 benchmarked with respect to the prediction of the slope in the outer assemblies?

Response to Question 1

The CASMO-4 methodology utilizes the same NRC-approved in-house methodology applied in our previous CASMO-3 calculations. This is the same methodology generally utilized by the industry. The CASMO-4/SIMULATE-3 methodology was benchmarked against measured assembly powers for cycles 12, 13, and 14. The rhodium reaction rates and pin-to-box factors are supplied by CASMO-4/SIMULATE-3. The rhodium reaction rates are used to convert incore detector fluxes into corresponding assembly powers. CASMO-4 and CASMO-3 produce similar reaction rates. The pin-to-box factors are based on SIMULATE-3 pin power reconstruction using CASMO-4 local peaking factors.

Since the industry is unable to benchmark any codes against measured pin powers within our reactors because these measurements are not available, critical experiments using small reactors is the only option. Therefore, pin power distributions across the outer assemblies are implicitly verified through this benchmarking process. The SIMULATE-3 pin power reconstruction is benchmarked against six B&W Critical Experiments. These six cores are the industry standard for benchmarking pin powers, and are comprised of three gadolinia cores and three non-gadolinia cores. As expected, CASMO-4 performed significantly better than CASMO-3 on the gadolinia cores, especially around the gadolinia pins. CASMO-4 was written in part to improve gadolinia modeling. Gadolinia has been used as a burnable absorber at Palisades since cycle 3.

The SIMULATE-3 reflector model is the same for both CASMO-3 and CASMO-4 methods. Therefore, changes in the radial power distributions from CASMO-3 to CASMO-4, which led to lower pin powers on the periphery, can be attributed to the improved gadolinia modeling.

The Palisades Incore Monitoring System (PIDAL) was developed by Consumers Energy and was approved by the NRC as Amendment No. 144 to License No. DPR-20 dated April 3, 1992. This Incore Monitoring System methodology utilized vendor supplied rhodium reaction rates and pin-to-box factors calculated using CASMO-2E/PDQ. The first update

to our Incore Monitoring System was approved by NRC on May 6, 1997[1]. This revised methodology utilizes rhodium reaction rates and pin-to-box factors calculated using CASMO-3/SIMULATE-3. The second update to our Incore Monitoring System was submitted for NRC approval on April 21, 2000[2]. This updated methodology utilizes rhodium reaction rates and pin-to-box factors calculated using CASMO-4/SIMULATE-3. This submittal is under review.

---

[1] NRC Letter to Thomas C. Bordine, "Approval of Revision to PIDAL In-core Monitoring Code" (TAC No. M96288) dated May 6, 1997.

[2] Consumers Energy Letter to NRC, "Request for Approval of Revision to Incore Monitoring Code (PIDAL-3)" dated April 21, 2000 (TAC No. MA8695).

Reply to Request for Additional Information Regarding Reactor Pressure Vessel Neutron Fluence Evaluation

NRC Question 2

The 3-D synthesis model enables the prediction of the fast neutron flux in locations off the core's mid-plane. The data from the core top and core bottom are not counted in the final evaluation. Performance at these locations seems to be poor--see for example, Table 4.3-11. Similar results have been obtained elsewhere--for examples, WCAP-14284 and WCAP-12794. One of the stated objectives of the 3-D synthesis was to "...address concerns regarding the axial leakage effects..." Since no attempt was made to justify these deviations or to address the leakage concerns, what is the purpose of these measurements?

Response to Question 2

As discussed in Section 3.1 (page 3-1) of WCAP 15353, use of a 3-D synthesis model as described in draft Regulatory Guide DG-1053 improves the accuracy of core mid-plane fast flux calculations by incorporating the effects of axial neutron scattering. It does not provide a definitive estimate of axial neutron leakage at the top and bottom (edges) of the core. Core top and bottom data were provided in Table 4.3-11 (and others) only for completeness since it was derived from the reactor cavity measurement program. Top and bottom core data were not used to adjust the calculated core mid-plane fast neutron flux which is of interest from a fluence perspective.

The neutron transport analyses described in WCAP-14284 and WCAP-12794 did not include the application of the 3-D synthesis approach. Therefore, direct comparisons of off-midplane results from these reports with the results from the Palisades application in WCAP-15353 can not be made.

The intent of the reactor cavity measurement program at the Palisades plant was to obtain a significant amount of data primarily over the active height of the core for comparison with calculation. The calculated neutron environment near the extreme top and bottom of the active fuel are highly sensitive to detector positioning as well as to axial power distribution effects at the edges of the fuel. Furthermore, the axial extent of the analytical model above and below the active fuel may also significantly impact the neutron spectrum. In particular, for a wide reactor cavity like Palisades, the portion of the ex-vessel dosimetry which lies at the axial edges of the active core and beyond are influenced by:

- the composition and extent of axial reflectors and the surrounding reactor internal components/structures;
- structures in the reactor cavity, e.g., loop nozzles, vessel supports, et cetera;

- the use of core midplane compositions and materials to represent the axial extremes of the fuel; and
- water density differences.

Thus, the calculational uncertainty would be expected to vary axially. The uncertainty would be the smallest at the core midplane location and increase towards both the bottom and top of the active fuel height. These effects are far less important opposite the central region of the reactor core. Therefore, in the Palisades application, only the midplane measurements were presented for comparison with the beltline region computations.

As a confirmatory check, however, it is of some interest to compare the Palisades calculated results with dosimetry results within the context of the calculational uncertainty of about 14%. If it is assumed that the calculated values represent an unbiased estimate with a standard deviation of 14%, the following distribution of LSA/C values for the neutron flux (E > 1.0 MeV) are observed for the 22 in-vessel and ex-vessel measurement locations:

	Expected Fraction	Expected Number	Observed Fraction	Observed Number
Nominal $\pm 1\sigma$	0.67	15	0.86	19
Nominal $\pm 2\sigma$	0.95	21	0.95	21
Nominal $\pm 3\sigma$	1.00	22	1.00	22

The data set is seen to exhibit an approximately normal distribution with respect to the calculational uncertainty of 14%. No data point lies more than 3σ from the nominal calculated value.

Even if the calculation is assumed to represent an unbiased estimate with a standard deviation as low as 10%, the following data table illustrates the same conclusion:

	Expected Fraction	Expected Number	Observed Fraction	Observed Number
Nominal $\pm 1\sigma$	0.67	15	0.77	17
Nominal $\pm 2\sigma$	0.95	21	0.95	21
Nominal $\pm 3\sigma$	1.00	22	1.00	22

No data point lies more than 3σ from the nominal calculated value.

Thus, the data set as a whole, including the off midplane locations in the reactor cavity, supports the overall uncertainty estimate for the Palisades fluence calculations.

Reply to Request for Additional Information Regarding Reactor Pressure Vessel Neutron Fluence Evaluation

NRC Question 3

On page 1-2, it is stated that in order to minimize the uncertainties, neutron transport calculations must be compared to industry-wide power reactor data bases. Where are the results of these comparisons?

Response to Question 3

Over the operating lifetime of power reactors, surveillance capsules are periodically withdrawn to provide materials data as well as neutron dosimetry applicable to the specific reactor. These dosimetry evaluations afford the opportunity for benchmarking of plant specific neutron transport calculations. While a plant-specific conclusion about uncertainties can not be drawn from this comparison, it can show whether reasonable consistency exists. The discussion below shows that when this comparison is performed for Palisades, the results are reasonably consistent with other relevant data.

In Table 3-1 below, a series of plant-specific calculations using the BUGLE-96 cross-section library is compared with the values of $\phi(E > 1.0\ \text{MeV})$ determined from the least squares evaluation of the individual dosimetry sensor sets. This table represents the entire population of surveillance capsules analyzed to date by Westinghouse using the BUGLE-96 cross sections. The in-vessel surveillance capsule database provided in Table 3-1 consists of 43 surveillance capsules removed from 14 reactors of similar design. This subset of Westinghouse reactors has the same nominal core configuration, reactor internals geometry, and pressure vessel inner radius and thickness. These reactors operate at similar core power levels and exhibit similar reactor coolant temperatures. The data set consists of as few as one and as many as six dosimetry data sets from a single reactor.

The comparisons shown in Table 3-1 represent an evaluation of the database as a whole. Based on these comparisons, the average LSA/C ratio for the entire database is seen to be 0.950 with a 1σ standard deviation of 6%. The individual sensor set LSA/C ratios range from a low of 0.817 to a high of 1.086. Thus, all of the individual sensor set comparisons fall within approximately $\pm$ 14% relative to the average value of 0.950. This range is also illustrated in Table 3-1 through a comparison of the least squares adjusted $\phi(E > 1.0\ \text{MeV})$ with the calculated values after removal of the 0.950 LSA/C ratio.

Table 5.1-1 (page 5-3) of WCAP 15353 contains the LSA/C values for the five internal (in-vessel) capsules withdrawn from Palisades to date. The Palisades values of LSA/C for the five capsules fall within the range 0.955 to 1.078. These values are bounded by the LSA/C values presented in Table 3-1. While a specific conclusion about uncertainties can not be drawn from this comparison, it does show that reasonable consistency exists.

Reply to Request for Additional Information Regarding Reactor Pressure Vessel Neutron Fluence Evaluation

Table 3-1: Comparison of Calculated and Least Squares Adjusted ϕ(E > 1.0 MeV) 4-Loop Plant In-Vessel Database

Capsule	Least Squares Adjusted ϕ(E>1.0 MeV) [n/cm^2-s]	Calculated ϕ(E>1.0 MeV) [n/cm^2-s]	[LSA]/[C]	K * Calculated ϕ(E>1.0 MeV) [n/cm^2-s]	[LSA]/[K*C]
5-U	1.10e+11	1.09e+11	1.012	1.03e+11	1.065
5-X	8.74e+10	9.74e+10	0.898	9.25e+10	0.945
5-Y	6.15e+10	7.53e+10	0.817	7.16e+10	0.860
18-X	1.05e+11	1.11e+11	0.939	1.06e+11	0.988
18-U	9.99e+10	1.06e+11	0.943	1.01e+11	0.993
18-Z	9.87e+10	1.04e+11	0.948	9.89e+10	0.998
18-W	9.67e+10	1.01e+11	0.958	9.59e+10	1.008
18-V	9.45e+10	9.88e+10	0.957	9.39e+10	1.007
18-Y	8.32e+10	9.11e+10	0.913	8.66e+10	0.961
19-U	1.09e+11	1.10e+11	0.997	1.04e+11	1.049
19-X	9.09e+10	8.36e+10	1.086	7.95e+10	1.143
19-Y	7.44e+10	8.31e+10	0.895	7.90e+10	0.942
20-U	1.11e+11	1.11e+11	1.008	1.05e+11	1.060
20-Y	8.36e+10	8.66e+10	0.965	8.23e+10	1.015
21-U	1.04e+11	1.03e+11	1.004	9.81e+10	1.057
21-Y	8.41e+10	8.69e+10	0.968	8.26e+10	1.018
21-V	7.54e+10	8.04e+10	0.938	7.64e+10	0.987
22-V	9.63e+10	9.20e+10	1.046	8.75e+10	1.101
22-Y	7.05e+10	8.05e+10	0.876	7.65e+10	0.921
23-U	1.24e+11	1.17e+11	1.052	1.12e+11	1.108
23-X	1.03e+11	1.10e+11	0.937	1.05e+11	0.986
23-Z	9.52e+10	1.04e+11	0.916	9.87e+10	0.964
23-V	8.38e+10	9.07e+10	0.924	8.62e+10	0.972
23-Y	8.18e+10	8.84e+10	0.925	8.40e+10	0.974
24-U	1.27e+11	1.23e+11	1.032	1.17e+11	1.086
25-U	9.51e+10	1.07e+11	0.887	1.02e+11	0.933
25-Y	7.72e+10	8.72e+10	0.886	8.28e+10	0.932
25-V	7.40e+10	8.06e+10	0.917	7.66e+10	0.965
26-Z	1.28e+10	1.20e+11	1.069	1.14e+11	1.125
26-U	7.64e+10	8.34e+10	0.917	7.92e+10	0.965
26-X	8.35e+10	8.34e+10	1.001	7.92e+10	1.054
26-Y	7.97e+10	8.40e+10	0.949	7.98e+10	0.999
26-V	7.23e+10	7.97e+10	0.907	7.57e+10	0.954
27-U	9.81e+10	1.11e+11	0.882	1.06e+11	0.928
27-X	8.20e+10	8.80e+10	0.932	8.36e+10	0.981
27-W	7.21e+10	8.34e+10	0.865	7.92e+10	0.910
28-U	1.17e+11	1.20e+11	0.981	1.14e+11	1.032
28-Y	8.14e+10	8.44e+10	0.964	8.02e+10	1.015
29-U	1.04e+11	1.06e+11	0.981	1.01e+11	1.032
29-Y	8.46e+10	9.04e+10	0.936	8.59e+10	0.985
29-V	8.08e+10	8.44e+10	0.958	8.02e+10	1.008
30-U	1.04e+11	1.11e+11	0.936	1.06e+11	0.985
30-W	8.16e+10	8.69e+10	0.938	8.26e+10	0.987
[LSA]/[C] Ratio - K			0.950		1.00
% standard deviation			6		6

Reply to Request for Additional Information Regarding Reactor Pressure Vessel Neutron Fluence Evaluation

NRC Question 4

On page 2-1, it is stated that "At each of the azimuthal locations selected for core midplane spectra measurements..." How and where in WCAP-15353 were these spectral measurements analyzed and how were they used?

Response to Question 4

The results of the least squares adjustment were not used in any way to change or bias the absolute neutron transport calculations performed for the Palisades reactor pressure vessel.

In WCAP-15353, the term "spectra measurements" refers to the use of the multiple foil sensor sets that provide full spectral coverage in the fast neutron energy range. The availability of the complete foil set, as opposed to only gradient chain, permits the application of the least squares evaluations to determine a best-fit spectra at these specific measurement locations. The analyses associated with these data sets is discussed in Section 4.0 of WCAP-15353.

The results of these evaluations and the subsequent comparison to calculations provided in Table 5.1-1 (page 5-3) of WCAP-15353 were used solely to demonstrate that the range of LSA/C comparisons were consistent with the uncertainty in the calculated values. That is, the results were used to validate the plant-specific calculation.

Reply to Request for Additional Information Regarding Reactor Pressure Vessel Neutron Fluence Evaluation

NRC Question 5 – Part (1)

On page 2-3, it is stated that high purity iron and cobalt foils provide a check on the chemical analysis of Type 304 stainless steel:

(1) Where is this check carried out and what was the conclusion?

Response to Question 5 - Part (1)

The primary means of determining the composition of the stainless steel gradient chains is by chemical means using certified NIST samples as a control. The data sheets from these analyses are provided in the appendices to WCAP-15353. The data obtained from this method were used in all evaluations of the gradient chains.

The comparison of pure foil reaction rates with the corresponding reaction rates from the gradient measurements near the core midplane merely provides another check on the counting and data evaluation processes. That is, a serious disagreement between reaction rates obtained from the high-purity foils and the stainless steel chains would require a review of the counting data and analysis procedure; and, possibly, rejection of a measurement. Comparisons of the gradient chain measurements with the high purity foil data can be made using the reaction rate measurements given in Section 4.0 of WCAP-15353.

The reaction rates of the high purity foils did show reasonable consistency with the gradient chain measurements. This provided independent confirmation that the dosimetry counting of the foils and chemical analysis of the gradient chains were correctly performed.

NRC Question 5 – Part (2)

(2) Given the magnitude of uncertainty associated with dosimetry, is dosimetry a proper means to check chemical composition?

Response to Question 5 - Part (2)

We concur that dosimetry is not a proper means to determine the chemical composition of a substance. As discussed in the response to Part (1) above, data from chemical analyses were used in all evaluations of the gradient chains.

Reply to Request for Additional Information Regarding Reactor Pressure Vessel Neutron Fluence Evaluation

NRC Question 6

On page XVII, the azimuthal reactor pressure vessel fluence values at the end of cycle 14 are listed and the cycle 15 flux is presented in Table 6.1-15. Please provide the cycle 15 and the remaining effective full power seconds to allow the determination of the proposed fluence value at the end of license (including any currently proposed extension of the license's expiration date).

Response to Question 6

Cycle 15 estimated Effective Full Power Seconds (EFPS) operating time:
EFPS = 444.3 EFPD x 24 hrs/day x 3600 sec/hr
= 3.839×10^7 seconds

Total estimated effective full power operating time for the current license expiration date of March 14, 2007:

EFPS = (EOL - EOC14) x 365.25 day/yr x 24 hr/day x 3600 sec/hr x 0.887 (capacity factor)
= (2007.20 - 1999.95) x 365.25 x 24 x 3600 x 0.887
= 2.029×10^8 seconds

Total estimated effective full power operating time for the proposed license expiration date of March 24, 2011:

EFPS = (2011.23 - 1999.95) x 365.25 day/yr x 24 hr/day x 3600 sec/hr x 0.887 (capacity factor)
= 3.157×10^8 seconds

Reply to Request for Additional Information Regarding Reactor Pressure Vessel Neutron Fluence Evaluation

NRC Question 7a

On page 3-4, it is reported that water density effects in the outer fuel assemblies were calculated using the thermal-hydraulic model in SIMULATE. What are the results of this analysis and what temperature was used for the calculation of the water density?

Response to Question 7a

The average temperature of the 29 peripheral bundles was used in the DORT calculation. The following table summarizes the average peripheral temperature and density for Cycle 1 through Cycle 15. For a detailed discussion of the calculation of the temperature used in the DORT calculation, see Section 7.3 of this response below.

Cycle	Peripheral Average Temperature $T_{p,ave}$ [°F]	Peripheral Average Density $\rho_{p,ave}$ [g/cm^3]
1	543.4	0.753
2	549.0	0.749
3	558.4	0.739
4	560.2	0.737
5	561.1	0.736
6	561.1	0.736
7	561.1	0.736
8	555.2	0.743
9	556.2	0.742
10	555.2	0.743
11	552.4	0.746
12	552.4	0.746
13	554.3	0.744
14	556.2	0.742
15	556.2	0.742

NRC Question 7b

Was mixing accounted for in SIMULATE?

Response to Question 7b

Mixing was not accounted for in SIMULATE-3. Instead a conservative value for water density was derived by averaging the water densities within the assemblies located in the three outermost rows. This average density is lower than the density in the outermost row, and higher than in the innermost row. The averaged density is also lower than the density calculated by SIMULATE-3 for the outermost row of assemblies, and is, therefore, conservative to use in this analysis. For a discussion of the thermal-hydraulic model of SIMULATE-3, see Section 7.2 of this response below.

NRC Question 7c

Could another code like THINC produce more accurate results?

Response to Question 7c

A code such as THINC (which takes into account the effects of mixing in between individual assemblies) would be able to predict the localized mixing in the core more accurately than SIMULATE-3. As discussed above in the response to 7b, however, its use would not affect the calculated water density used in the fluence calculation. For a detailed discussion of measured and calculated core exit temperatures vs. assembly powers, please refer to Sections 7.3 and 7.4 below.

7.1 SUMMARY

The cross-flow between assemblies in the Palisades core geometry is very small due to the existence of wide water gaps between assemblies. The thermal-hydraulic model of SIMULATE-3 calculates the coolant enthalpy distribution by a simple heat balance of the enthalpy at the inlet of a node, the heat generated within the node, and the enthalpy at the outlet of a node. Hence, provided that the mass flow rate is known, the SIMULATE-3 code predicts the measured temperature distribution very well. The benefit of the SIMULATE-3 code is that the method of determining the temperature in the peripheral assemblies is consistent for all cycles as well as being consistent with the neutronics solution for each burnup step within the cycle.

7.2 SIMULATE-3 THERMAL-HYDRAULIC MODEL

The thermal-hydraulic model in SIMULATE-3 is a simple heat balance model which makes the following assumptions [SIMULATE-3 Methodology: Advanced Three-Dimensional Two-Group Reactor Analysis Code, STUDSVIK/SOA-95/18]:

- The coolant inlet flow and temperature distributions are known.
- Coolant flow is in parallel channels, cross flow is ignored, and the core exit water temperature condition remains subcooled.
- Power produced by fuel rods within a node is also deposited in the coolant in that node.
- The pressure drop across the core is assumed to be negligible, and all water properties are evaluated at a single pressure.

These assumptions imply that the coolant enthalpy distribution can be calculated by a simple heat balance of the enthalpy at the inlet of a node, the heat generated within the node, and the enthalpy at the outlet of a node. The node-average density is calculated by evaluating the state properties of water at the average of the node inlet and outlet enthalpies. The state calculation is based on interpolation of data from the ASME Steam Tables or directly via an ASME Steam Table evaluation.

7.3 CALCULATION OF ASSEMBLY TEMPERATURES USING SIMULATE-3

The cycle-specific temperature of the coolant is calculated using the average temperature for the individual assemblies located in the three outer rows in the quarter core. The individual assembly temperatures are calculated using SIMULATE-3. Predetermined inlet temperatures and core mass flow rates are utilized as input parameters to this code. The neutronics part of the code calculates the individual assembly powers using neutron cross-sections developed in the CASMO-4 code. Considering the above assumptions, the temperature increase in a fuel assembly in the core is calculated using the following equation:

$$m_A \, c_p \, \Delta T = Q_A \, 3.412 \times 10^6 \qquad (7\text{-}1)$$

where:

m_A = Mass flow rate per assembly [lb_m/hr] = $m_{core}/204$
c_p = Specific heat of water [BTU/(lb_m-°F)]
ΔT = Temperature increase [°F] = $T_{out} - T_{in}$
Q_A = Assembly power [MW]

As discussed in STUDSVIK/SOA-95/18, SIMULATE-3 uses a nodalized version of equation (7-1). The SIMULATE-3 model used by Palisades for calculating the temperature has 25 axial nodes. The axially collapsed average temperature is utilized to determine the core midplane density distribution.

At Palisades, a uniform mass flow rate and temperature distribution is assumed at the inlet of the core. Prior to initial plant startup, Battelle Memorial Institute conducted 1/5 scale model flow tests of the Palisades reactor vessel. These flow tests were conducted with air. The results were summarized in Report No. CEND-358, "Final Report on Studies of Flow in a 1/5 Scale Model of the Palisades PWR," dated April 1969. These tests showed that the mass flow distribution is approximately uniform except in the peripheral fuel assemblies which are located furthest away from the cold legs (also called "the flats", which is the region around the 0° and 90° welds). Flows in these regions were approximately 5% less than the average assembly.

Assuming a uniform mass flow rate distribution in the core, a linear relationship between the assembly power (Q_A) and temperature increase (ΔT) applies as follows:

$$\Delta T = A\, Q_A \qquad (7\text{-}2)$$

where,

$$A\ [°F/MW] = 204\ [\text{Assemblies}] * 3.412 \times 10^6\ [(BTU/hr)/MW] / (m_{core}\ [lb_m/hr]\ c_p\ [BTU/lb_m\text{-}°F])$$

The value of A varies from cycle to cycle.

The full power core inlet temperature was determined using a cycle specific inlet temperature vs. power curve. Measured data was used for determining the core inlet temperature for the early cycles. The core inlet temperatures in the earlier cycles differs from the inlet temperature program currently used in the operation of the plant.

The core mass flow rate is determined using measured data for each cycle from Technical Specifications Surveillance Test RT-118, "PCS Calorimetric Mass Flow Determination".

Table 7-1 shows the thermal hydraulic input parameters and the SIMULATE-3 calculated peripheral temperatures and densities for each cycle. Table 7-3 shows the calculated axially averaged core densities and temperatures for each assembly for Cycle 14. These axially collapsed densities and temperatures closely correspond to the actual midplane densities due to the axial core power shape. The core material density used in the DORT

fluence calculation is calculated using the average density of the 29 peripheral assemblies (identified by the color gray in Table 7-3).

The density of the bypass flow between the core shroud and the core barrel ('bypass density') is calculated by taking the average of the inlet density and the average density in the 12 peripheral assemblies (identified by bold font in Table 7-3), i.e., $\rho_{bypass} = ½(\rho_{inlet} + \rho_{12assem})$. Table 7-2 summarizes the bypass temperature and density for Cycles 1 through 15.

Table 7-1: SIMULATE-3 Thermal-Hydraulic Calculation Summary

Cycle	PCS Pressure P [psia]	Core Mass Flow Rate m_{core} [lb_m/hr]	Coolant Inlet Temperature T_{inlet} [°F]	Coolant Inlet Density ρ_{inlet} [g/cm^3]	Peripheral Average Temperature $T_{p,ave}$ [°F]	Peripheral Average Density $\rho_{p,ave}$ [g/cm^3]
1	1840	137.7E+06	523	0.773	543.4	0.753
2	2010	137.7E+06	529	0.769	549.0	0.749
3	2010	137.7E+06	534	0.764	558.4	0.739
4	2010	137.7E+06	536	0.762	560.2	0.737
5	2010	137.7E+06	536	0.762	561.1	0.736
6	2010	137.7E+06	536	0.762	561.1	0.736
7	2010	137.7E+06	536	0.762	561.1	0.736
8	2060	137.7E+06	537	0.761	555.2	0.743
9	2060	142.9E+06	534	0.765	556.2	0.742
10	2060	142.3E+06	534	0.765	555.2	0.743
11	2060	141.6E+06	533	0.766	552.4	0.746
12	2060	141.0E+06	534	0.765	552.4	0.746
13	2060	142.3E+06	536	0.763	554.3	0.744
14	2060	141.0E+06	537	0.762	556.2	0.742
15	2060	141.0E+06	537	0.762	556.2	0.742

Table 7-2: Calculated Bypass Temperature and Density for Cycles 1 through 15

Cycle	Bypass Temperature, T_{BYPASS} [°F]	Bypass Density [g/cm^3]
1	531.4	0.765
2	536.3	0.761
3	545.2	0.753
4	547.1	0.751
5	547.1	0.751
6	547.1	0.751
7	547.1	0.751
8	542.8	0.756
9	538.8	0.760
10	537.8	0.761
11	536.8	0.762
12	537.8	0.761
13	538.8	0.760
14	540.8	0.758
15	539.8	0.759

Table 7-3: Cycle 14 MOC Quarter Core Assembly Water Densities and Temperatures from SIMULATE-3

Axially Averaged (Midplane) Quarter Core Water Density by Assembly, [g/cm^3]

	9	10	11	12	13	14	15	16
9	0.727	0.729	0.732	0.720	0.727	0.731	0.738	**0.754**
10	0.721	0.727	0.721	0.730	0.720	0.731	0.733	**0.754**
11	0.732	0.721	0.731	0.720	0.728	0.725	0.746	**0.757**
12	0.727	0.732	0.721	0.732	0.724	0.740	**0.753**	
13	0.728	0.720	0.728	0.724	0.744	**0.752**	**0.758**	
14	0.724	0.730	0.724	0.739	**0.752**			
15	0.739	0.732	0.745	**0.753**	**0.758**			
16	**0.754**	**0.753**	**0.756**					

Peripheral Average Density: 0.742 g/cc

Axially Averaged (Midplane) Quarter Core Water Temperature by Assembly, [°F]

	9	10	11	12	13	14	15	16
9	569.5	567.8	566.9	575.5	569.5	566.1	559.8	**544.7**
10	574.6	569.5	574.6	566.9	575.5	566.1	564.3	**544.7**
11	566.9	574.6	566.1	575.5	568.7	571.3	552.4	**541.7**
12	569.5	566.9	574.6	566.9	572.1	558.0	**545.7**	
13	568.7	575.5	568.7	572.1	554.3	**546.7**	**540.7**	
14	572.1	566.9	572.1	558.9	**546.7**			
15	558.9	565.2	553.4	**545.7**	**540.7**			
16	**544.7**	**545.7**	**542.7**					

Peripheral Average Temperature: 556.2 °F

7.4 MODELING OF MIXING EFFECTS

Mixing is not accounted for in SIMULATE-3, but this is conservatively addressed by averaging the water densities in the 29 peripheral assemblies to determine the density to be used in the fluence calculations. Therefore, precise modeling of mixing is not necessary.

Comparisons to measured in-core temperatures and assembly powers show that SIMULATE-3 adequately predicts the temperatures in the assemblies where core exit temperature (CET) measurements are available. The individual assembly temperatures and powers calculated by SIMULATE-3 for Cycle 14 MOC burnup conditions were

compared to in-core measurements of the assembly power and temperatures from various burnup stages of Cycle 14. Figure 7-1 below shows that the calculated values represent the measured values well. Peripheral mixing should not be different from the center since the core geometry is maintained. The present in-core measurement layout in the Palisades core geometry does not allow the peripheral assemblies to be measured; therefore, the interpolation of measured data to the lower-powered assemblies is currently precluded. To insure that adequate mixing effects have been taken into account in the core periphery, the calculated densities in the 29 outermost assemblies were averaged to produce the material properties of the coolant.

Figure 7-1: Measured and Calculated Assembly Powers vs. Temperature Increase for Cycle 14

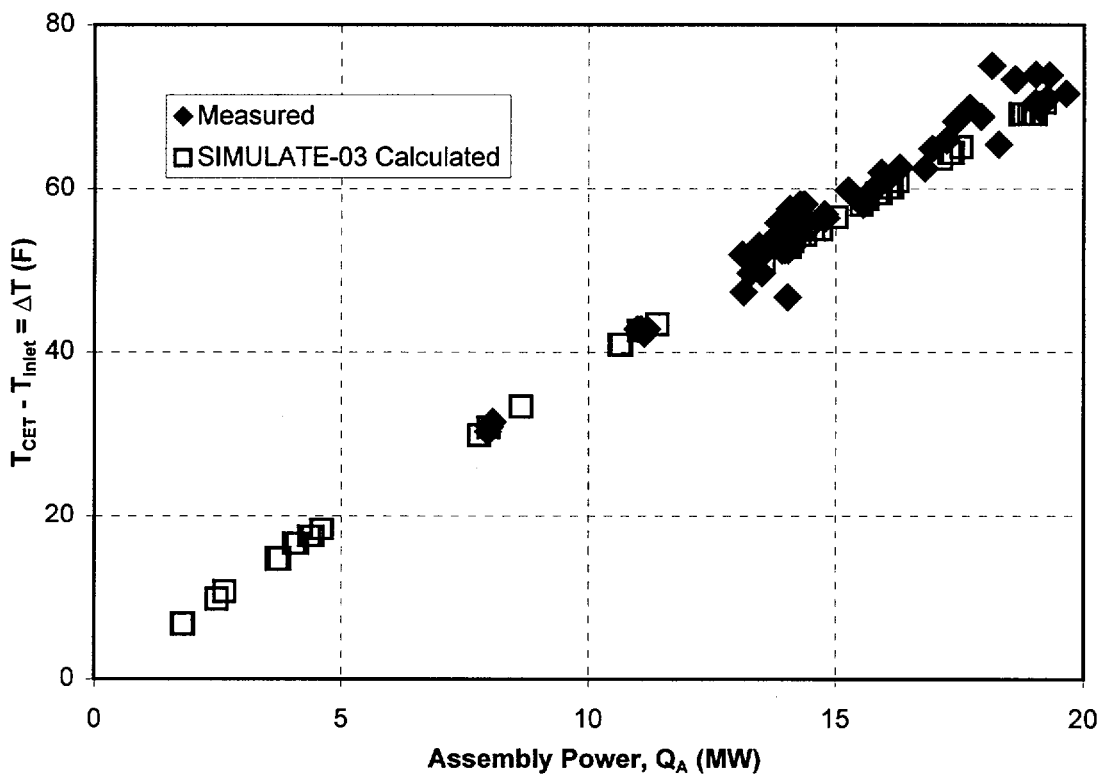

In the DORT fluence calculation, the density in the three peripheral rows of assemblies is averaged to yield the peripheral core water density. By averaging the densities, a uniform mixing among these assemblies is assumed. The individual assembly temperatures are calculated by SIMULATE-3. The averaging of densities in the core periphery in the DORT

model is conservative since there is a steep temperature gradient over the three peripheral rows of assemblies. The peripheral assemblies in the outermost row contribute the most to the fluence in the reactor vessel. This is due to the proximity to the vessel in comparison to the other rows, and also the amount of coolant in between the neutron source (assemblies) and the vessel. Using this three-row average value as the coolant temperature surrounding the outermost row of assemblies provides a temperature that is significantly higher than the specific value calculated by SIMULATE-3 for a peripheral assembly. A higher temperature leads to a lower density, which in turn leads to a lower macroscopic scattering cross-section of the coolant and a reduced calculated slow-down of the fast neutrons.

Therefore, while the THINC code would be able to predict the mixing in the core more accurately, its use would not change the resulting fast neutron flux utilized in the fluence calculation.

Reply to Request for Additional Information Regarding Reactor Pressure Vessel Neutron Fluence Evaluation

NRC Question 8

What was the size of the photofission correction reported on page 3-15? Was the associated γ-flux calculated?

Response to Question 8

The location dependent photo-fission correction terms that were applied to the $^{238}U(n,f)$ and $^{237}Np(n,f)$ measured reaction rates are identified in Table 8.1. It should be recognized that these photo-fission corrections were obtained from the forward transport calculations that supported WCAP-15353.

Table 8.1

	^{238}U (γ,f) Correction	^{237}Np(γ,f) Correction
Vessel Capsule		
A240	No U Sensor	No Np Sensor
SA60	0.971	0.984
W290	0.881	0.924
W290-9	0.881	0.924
W110	No U Sensor	No Np Sensor
Cavity Dosimetry		
6°	0.979	0.996
16°	0.981	0.996
26°	0.978	0.995
36°	0.973	0.995
39°	0.973	0.995
24°	0.978	0.995

Both the neutron and photon fluxes were determined in the forward transport calculations. These calculations were performed using a total of sixty-seven energy groups where the neutron energy-group structure was contained in groups 1 through 47 and the photon energy-group structure was in groups 48 through 67.

Reply to Request for Additional Information Regarding Reactor Pressure Vessel Neutron Fluence Evaluation

NRC Question 9

On page 3-15, it is stated that FERRET has "...assigned uncertainties and correlations..." What are the values and why are they relevant to this application? On page 3-18, it is stated that the values are "liberal enough" to fit the measured data for all practical applications. Are these values the product of judgement and selection or the product of some arithmetic or mathematical operation? These uncertainty assignments are stated to be a product of FERRET applications, but page 3-17 appears to indicate that they originated in Maerker's LEPRICON. Please clarify.

Response to Question 9

The predicted pressure vessel fluence that was generated in WCAP-15353 for Palisades was based solely on the results of the absolute transport calculations. The least squares adjustment was not used to derive the projected vessel fluence and was only provided for comparison with our prior reports and submittals. The results from FERRET, therefore, are not used for the current determination of reactor vessel fluence.

In the interest of completeness a theoretical discussion is provided in Attachment 2 which responds to this question.

Reply to Request for Additional Information Regarding Reactor Pressure Vessel Neutron Fluence Evaluation

NRC Question 10

In Tables 4.2-6 to 4.2-8, 4.2-13 to 4.3-15, etc., the actual location of the foils and chains do not have the symmetry implied by their first quadrant equivalent (FQE). What is the meaning of the average FQE 30°?

Response to Question 10

The subject tables are not utilized in the determination of the Palisades reactor vessel fluence. The predicted pressure vessel fluence that was generated in WCAP-15353 was based solely on the results of the absolute transport calculations. The least squares adjustment was not used to derive the projected vessel fluence and was only provided for comparison with our prior reports and submittals. The information in these tables, therefore, is not applicable to the current determination of reactor vessel fluence.

In the interest of completeness a theoretical discussion is provided in Attachment 2 which responds to this question.

Reply to Request for Additional Information Regarding Reactor Pressure Vessel Neutron Fluence Evaluation

NRC Question 11

In Tables 4.3-1 to 4.3-22, the least squares adjusted value is frequently outside the range of measured and calculated values. Please explain why this is acceptable and why it is physically meaningful. The values of $^{59}Co(n,\gamma)$ and $^{59}Co(n,\gamma)$ Cd seem to be problematic (here as well as in other WCAPs). Why are these values acceptable and what are the acceptance criteria? What would be the effect if the $^{59}Co(n,\gamma)$ and $^{59}Co(n,\gamma)$ Cd reactions were eliminated?

Response to Question 11

The subject tables are not utilized in the determination of the Palisades reactor vessel fluence. The predicted pressure vessel fluence that was generated in WCAP-15353 was based solely on the results of the absolute transport calculations. The least squares adjustment was not used to derive the projected vessel fluence and was only provided for comparison with our prior reports and submittals. The information in these tables, therefore, is not applicable to the current determination of reactor vessel fluence.

In the interest of completeness a theoretical discussion is provided in Attachment 2 which responds to this question.

Reply to Request for Additional Information Regarding Reactor Pressure Vessel Neutron Fluence Evaluation

NRC Question 12

Table 4.3-11 (and to a lesser degree, Table 4.3-18) are out of range compared with the other measurements. Although they are not counted in the final value, they appear to be indicative of some calculational or measurement problem. Please explain.

Response to Question 12

The purpose of performing measurements over the entire active fuel height was to confirm that the peak flux location was near the midplane of the core. Core top and bottom data provided in Table 4.3-11 (and others) were provided only for completeness since it was derived from the reactor cavity measurement program. Top and bottom core data were not used to adjust the calculated core mid-plane fast neutron flux which is of interest from a fluence perspective.

The intent of the reactor cavity measurement program at the Palisades plant was to obtain a significant amount of data primarily over the active height of the core for comparison with calculation. The calculated neutron environment near the extreme top and bottom of the active fuel are highly sensitive to detector positioning as well as to axial power distribution effects at the edges of the fuel. Furthermore, the axial extent of the analytical model above and below the active fuel may also significantly impact the neutron spectrum. In particular, for a wide reactor cavity like Palisades, the portion of the ex-vessel dosimetry which lies at the axial edges of the active core and beyond are influenced by:

- the composition and extent of axial reflectors and the surrounding reactor internal components/structures;
- structures in the reactor cavity, e.g., loop nozzles, vessel supports, et cetera;
- the use of core midplane compositions and materials to represent the axial extremes of the fuel; and
- water density differences.

Thus, the calculational uncertainty would be expected to vary axially. The uncertainty would be the smallest at the midplane location and increase towards both the bottom and top of the active fuel height. These effects are far less important opposite the central region of the reactor core. Therefore, in the Palisades application, only the midplane measurements were presented for comparison with the beltline region computations.

Reply to Request for Additional Information Regarding Reactor Pressure Vessel Neutron Fluence Evaluation

NRC Question 13

The "M/C" values in Tables 4.3-1 to 4.3-22 give a direct comparison of the measured and calculated sensor reaction rates. What was the statistical basis for accepting or rejecting measurements for inclusion in the least squares adjustment procedure?

Response to Question 13

The subject tables are not utilized in the determination of the Palisades reactor vessel fluence. The predicted pressure vessel fluence that was generated in WCAP-15353 was based solely on the results of the absolute transport calculations. The least squares adjustment was not used to derive the projected vessel fluence and was only provided for comparison with our prior reports and submittals. The information in these tables, therefore, is not applicable to the current determination of reactor vessel fluence.

In the interest of completeness a theoretical discussion is provided in Attachment 2 which responds to this question.

Reply to Request for Additional Information Regarding Reactor Pressure Vessel Neutron Fluence Evaluation

NRC Question 14 – Part (1a)

Regarding Section 6.2 of WCAP-15353:

(1) What methods were used in the benchmark comparisons whose results are quoted on page 6-27?

Response to Question 14 – Part (1a)

PCA Analysis

The initial neutron transport analysis of the PCA 12/13 configuration was carried out using the conventional three-dimensional synthesis technique described below. That is, the evaluation consisted of two DORT two-dimensional discrete ordinates transport calculations, one in x,y geometry and one in y,z geometry, as well as a single one-dimensional DORT calculation in planar (y) geometry to synthesize a three-dimensional solution throughout the PCA simulator. The synthesis was carried out using the following relationship:

$$\phi_g(x,y,z) = \phi_g(x,y) * \frac{\phi_g(y,z)}{\phi_g(y)}$$

where,

$\phi_g(x,y,z)$ =	The group-g neutron flux at position x,y,z within the simulator geometry.
$\phi_g(x,y)$ =	The group-g neutron flux solution from the x,y DORT computation.
$\phi_g(y,z)$ =	The group-g neutron flux solution from the y,z DORT computation.
$\phi_g(y)$ =	The group-g neutron flux solution from the y DORT computation.

In this synthesis approach the ratio $[\phi_g(y,z)]/[\phi_g(y)]$ represents the energy and spatially dependent axial shape factor that accounts for the finite height of the PCA core as well as for the axial leakage effects introduced by the simulator geometry.

In the calculation of the PCA 12/13 configuration, all of the DORT computations were carried out in 67 energy groups (47 neutron, 20 gamma-ray) using a P_3 cross-section expansion and an S_8 order of angular quadrature. The analysis was carried out using the BUGLE-96 cross-section library.

The comparisons of the two-dimensional calculations with measured reaction rates showed a trend towards under-prediction with increased depth into the pressure vessel simulator. To test whether this trend was due to inadequacies in the transport cross-sections or in the application of the two-dimensional synthesis technique to the analysis of a small reactor

system, the PCA Analysis was repeated using the TORT three-dimensional discrete ordinates code in x,y,z geometry. The TORT analysis was also performed using the BUGLE-96 cross-section library with a P_3 scattering cross-section expansion and an S_8 order of angular quadrature. The use of the three-dimensional model substantially improved the agreement between calculation and measurement throughout the pressure vessel simulator.

H. B. Robinson Analysis

The neutron transport analysis of the H. B. Robinson benchmark configuration was also carried out using the conventional three-dimensional synthesis technique described below. That is, the evaluation consisted of two DORT two-dimensional discrete ordinates transport calculations, one in r,θ geometry and one in r,z geometry, as well as a single one-dimensional DORT calculation in cylindrical (r) geometry to synthesize a three-dimensional solution throughout the reactor geometry. The synthesis was carried out using the following relationship:

$$\phi_g(r,\theta,z) = \phi_g(r,\theta) * \frac{\phi_g(r,z)}{\phi_g(r)}$$

where,

$\phi_g(r,\theta,z)$ =	The group-g neutron flux at position r,θ,z within the reactor geometry.
$\phi_g(r,\theta)$ =	The group-g neutron flux solution from the r,θ DORT computation.
$\phi_g(r,z)$ =	The group-g neutron flux solution from the r,z DORT computation.
$\phi_g(r)$ =	The group-g neutron flux solution from the r DORT computation.

In the calculation of the H. B. Robinson benchmark configuration, all of the DORT computations were carried out in 67 energy groups (47 neutron, 20 gamma-ray) using a P_3 cross-section expansion and an S_8 order of angular quadrature. The analysis was carried out using the BUGLE-96 cross-section library.

NRC Question 14 – Part (1b)

(1b) What are the systematic components (i.e., bias) and the random components that result in the quoted 3% for each case?

Response to Question 14 – Part (1b):

The uncertainty assignment from the PCA comparisons was based on a comparison of the TORT calculations with least squares adjusted values of neutron flux (E > 1.0 MeV) for positions A1 through A7 in the pressure vessel simulator. This data comparison showed

an average LSA/C ratio for the neutron flux (E > 1.0 MeV) of 1.002 with a standard deviation of 2.3% for the seven data points. The range of LSA/C ratios was 0.97 to 1.03. This comparison was taken to confirm the basic BUGLE-96 neutron transport cross-sections and the discrete ordinates methodology produced an unbiased calculation within the 2.3% standard deviation. For the overall uncertainty estimate, a conservative value of 3% was taken and treated as a random component associated with transport cross-sections and basic transport methodology. As a further check on this assessment, comparisons were also made directly with individual sensor measured reaction rates at locations A1 through A7 of the simulator. These data comparisons show an average M/C ratio of 0.98 with a standard deviation of 3.5% for the 35 sample data set. The range of M/C ratios was 0.91 to 1.05.

The uncertainty assignment from the H. B. Robinson comparisons was based on a comparison of the DORT synthesis calculations with least squares adjusted values of neutron flux (E > 1.0 MeV) at both in-vessel and ex-vessel locations. This data comparison showed an average LSA/C ratio for the neutron flux (E > 1.0 MeV) of 1.005 with a standard deviation of 2.1% for the two data points. The range of LSA/C ratios was 0.99 to 1.02. This comparison was taken to confirm the basic BUGLE-96 neutron transport cross-sections and the discrete ordinates methodology along with the application of a power reactor geometric model and core source determination produced an unbiased calculation within the 2.1% standard deviation. For the overall uncertainty estimate, a conservative value of 3% was taken and treated as a random component associated with power reactor applications. As a further check on this assessment, comparisons were also made directly with individual sensor measured reaction rates at the in-vessel and ex-vessel locations. These data comparisons show an average M/C ratio of 1.03 with a standard deviation of 4.2% for the 11 sample data set. The range of M/C ratios was 0.95 to 1.11.

Although the effects of cross-section and basic transport methodology uncertainties are applicable to both the PCA and H. B. Robinson evaluations, there is no practical way to separate these effects from the power reactor geometric and source distribution uncertainties that impact only the H. B. Robinson analysis. Therefore, in the overall uncertainty evaluation, the 3% uncertainty from the PCA and the 3% uncertainty from the H. B. Robinson benchmark were conservatively treated as uncorrelated. This results in the largest uncertainty value.

Reply to Request for Additional Information Regarding Reactor Pressure Vessel Neutron Fluence Evaluation

NRC Question 14 – Part (2a)

(2a) What methods were used in the analytic sensitivity studies?
Response to Question 14 – Part (2a)

For the evaluation of the effect of uncertainties in the thickness of the reactor internals (core shroud and core support barrel), in the vessel cladding in the inner radius of the pressure vessel, and in the temperature of the reactor coolant, the results of two-dimensional r,θ DORT calculations were used to establish the perturbation effects associated with potential deviations in these input variables. The impact of uncertainties associated with the neutron source was assumed to be linear for all locations in the reactor geometry. It was further assumed that uncertainties associated with basic nuclear data are included in the uncertainties derived from the evaluations of the PCA and H.B. Robinson benchmarks.

NRC Question 14 – Part (2b)

(2b) What were the fluence sensitivity and the estimate of the expected uncertainty that gave the quoted results?

Response to Question 14 – Part (2b)

Uncertainty Source	Fluence Sensitivity	Estimated Uncertainty	Fluence Uncertainty
Core Source	1% df/% ds	10%	10%
Water Temperature	0.4% df/°F	7 °F	3%
Vessel Inner Radius	22% df/in	0.14 in	3%
Cladding Thickness	14% df/in	0.075 in	1%
Internals Tolerances	16% df/in	0.125 in	2%
Numerical Procedures			5%

In the above tabulation the term "df" refers to the change in fluence per unit parameter. The term "ds" refers to the change in unit source strength.

NRC Question 14 – Part (3a)

(3a) What is included under "Other Factors" and how was this uncertainty estimated?

Response to Question 14 – Part (3a)

The "Other Factors" category that appears as a separate entity in the uncertainty assessment performed for the Palisades fluence evaluation is simply a repository for all undefined or unknown items that could have affected the analysis. Although specific contributors are identified in the other categories (i.e., PCA benchmark comparisons, H. B. Robinson benchmark comparisons, and analytical sensitivity studies), it was deemed appropriate to consider a nonspecific source of uncertainty that is anticipated to be a minor contributor relative to the total calculated uncertainty. Engineering judgement was utilized to assign this nonspecific category an uncertainty value of 5% since this is between the benchmark problem uncertainties and the analytical sensitivity study uncertainty. It is also believed that this value is conservative since the uncertainty from all nonspecific sources should be less than the smallest uncertainty from any specific source (in this case, $\leq 3\%$).

NRC Question 14 – Part (3b)

(3b) Are there any correlations among the components?

Response to Question 14 – Part (3b)

There are no known correlations among the components; however, the potential exists for double counting to occur since an item from the "Other Factors" category could conceivably overlap with an item from the other three specific categories. This is not assumed, however, since the four categories were combined in quadrature to determine the overall uncertainty for the Palisades fluence evaluation.

NRC Question 14 – Part (4)

How have the benchmark uncertainties been incorporated into the overall calculated fluence uncertainty? Are there correlations?

Response to Question 14 – Part (4)

As indicated in WCAP-15353 and in the response to RAI 14 – Part (3b), the benchmark uncertainties were combined in quadrature with the "Analytical Sensitivity Studies" category and the "Other Factors" category to determine the overall calculated fluence uncertainty.

There are no known correlations among the components; however, the potential exists for double counting to occur since an item from the "Other Factors" category could conceivably overlap with an item from the other three specific categories. This is not assumed,

however, since the four categories were combined in quadrature to determine the overall uncertainty for the Palisades fluence evaluation.

NRC Question 14 – Part (5)

(5) Do the dosimeter evaluations in Figure 6.2-1 include the uncertainty in the flux spectrum after the least squares adjustment?

Response to Question 14 – Part (5)

No. Figure 6.2-1 of WCAP-15353 does not show the flux spectrum uncertainty after the least squares adjustment for each of the dosimetry samples that were analyzed for Palisades. However, this information is given in Figure 14.5-1 that is presented below.

Figure 14.5-1: Comparison of LSA Results to Calculation for Fast Neutron Flux (E > 1.0 MeV) with the Flux Spectrum Uncertainty Included

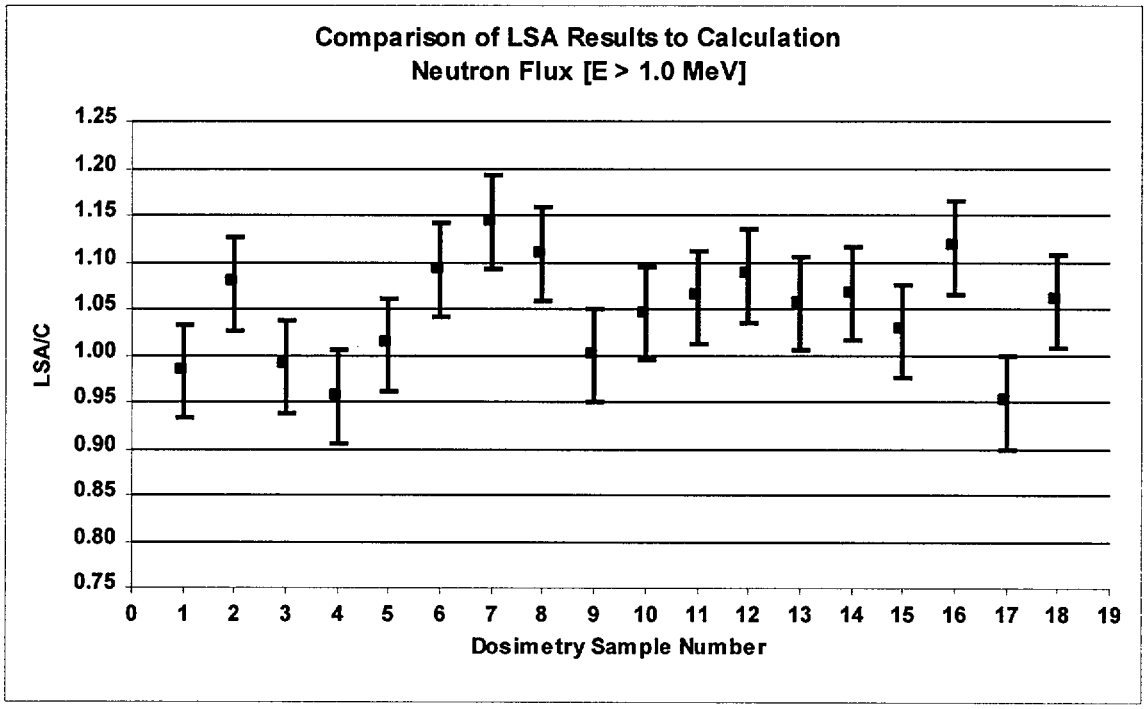

Reply to Request for Additional Information Regarding Reactor Pressure Vessel Neutron Fluence Evaluation

NRC Question 15*a*

What is the bottom line of your submittal dated February 21, 2000—(i.e., what is the projected calculated limiting-element inside-surface fluence value at the end of the current operating license, and for the currently proposed extension of the license's expiration date?)

Response to Question 15a

Fluence values are provided below. Each fluence is calculated using the fluence value from the end of cycle 14 (EOC 14) and the cycle 15 flux at the location of interest.

Estimated peak fluence for the current license expiration date of March 14, 2007:

ϕt = EOC 14 peak fluence + (Corresponding cycle 15 flux)(Time to license expiration)
= 1.533×10^{19} n/cm^2 + (1.673×10^{10} n/cm^2-sec)(2.029×10^8 sec)
= 1.873×10^{19} n/cm^2

Estimated fluence at the limiting axial weld for the current license expiration date of March 14, 2007:

ϕt = EOC 14 fluence at location + (Corresponding cycle 15 flux)(Time to license expiration)
= 1.158×10^{19} n/cm^2 + (1.058×10^{10} n/cm^2-sec)(2.029×10^8 sec)
= 1.373×10^{19} n/cm^2

Estimated peak fluence for the proposed license expiration date of March 24, 2011:

ϕt = EOC 14 peak fluence + (Corresponding cycle 15 flux)(Time to license expiration)
= 1.533×10^{19} n/cm^2 + (1.673×10^{10} n/cm^2-sec)(3.157×10^8 sec)
= 2.061×10^{19} n/cm^2

Estimated fluence at the limiting axial weld for the proposed license expiration date of March 24, 2011:

ϕt = EOC 14 fluence at location + (Corresponding cycle 15 flux)(Time to license expiration)
= 1.158×10^{19} n/cm^2 + (1.058×10^{10} n/cm^2-sec)(3.157×10^8 sec)
= 1.492×10^{19} n/cm^2

NRC Question 15b

What are the corresponding "measured" values?

Response to Question 15b

Although the synthesis calculations were performed in WCAP-15353, they were not utilized in conjunction with a bias factor since prior interactions with the NRC Staff have indicated a preference for utilizing the calculated results only. The least squares adjusted flux estimates are included in WCAP-15353 only to completely describe the calculational methodology changes that have been made relative to prior Palisades submittals. Input received from prior independent reviews[1] has suggested that it was inappropriate to include both the ex-vessel and in-vessel dosimetry results in determining a single plant-specific bias factor unless other actions are also taken. For example, one suggestion made was to perform a sensitivity study, either using adjoint transport calculations or the perturbation feature of the MCNP Monte Carlo code, that establishes a strong correlation between the neutron spectrum and the flux at the dosimetry and critical weld locations. Another suggestion that was made during past reviews was, in the absence of a sensitivity analysis which correlates the ex-vessel and in-vessel spectral shapes, to simply use the bias factors from the in-vessel surveillance capsule locations only. A third approach suggested in previous reviews was to utilize 2-D/1-D flux synthesis calculations in conjunction with a single LSA/C bias factor that was based on the combination of in-vessel and ex-vessel dosimetry.

Given the above options, if we were to adjust the above calculated fluences, we would use the average correction for the five in-vessel dosimetry capsules (see Table 5.1-1 on page 5-3 of WCAP 15353). The resulting value of this bias factor would be 1.003. Each estimated fluence listed in the response to 15a above would be multiplied by 1.003 to obtain the adjusted value.

---

[1]Haskell (Consumers) to NRC, "Docket 50-255 - License DPR-20 - Palisades Plant - Reactor Vessel - Independent Reviews of the Palisades Reactor Vessel Fluence Methodology," April 20, 1998.

Reply to Request for Additional Information Regarding Reactor Pressure Vessel Neutron Fluence Evaluation

NRC Question 15c

What is the projected reference temperature for pressurized thermal shock (RT_{PTS})?

Response to Question 15c

The projected RT_{PTS} for each of the reactor vessel beltline materials on March 14, 2007 is:

Component Identification	Heat #	EOL Fluence (n/cm²)	RT_{PTS} (°F)
2-112A/C	W5214	1.373×10^{19}	261
3-112A/C	W5214	1.373×10^{19}	261
	34B009	1.373×10^{19}	246
9-112	27204	1.873×10^{19}	275*
D-3803-1	C-1279	1.873×10^{19}	192
D-3803-2	A-0313	1.873×10^{19}	192
D-3803-3	C-1279	1.873×10^{19}	192
D-3804-1	C-1308A	1.873×10^{19}	185
D-3804-2	C-1308B	1.873×10^{19}	158
D-3804-3	B-5294	1.873×10^{19}	105

*circumferential weld subject to 300°F limit

Reply to Request for Additional Information Regarding Reactor Pressure Vessel Neutron Fluence Evaluation

The projected RT_{PTS} for each of the reactor vessel beltline materials on March 24, 2011 is:

Component Identification	Heat #	EOL Fluence (n/cm²)	RT_{PTS} (°F)
2-112A/C	W5214	1.492×10^{19}	266
3-112A/C	W5214	1.492×10^{19}	266
	34B009	1.492×10^{19}	251
9-112	27204	2.061×10^{19}	281*
D-3803-1	C-1279	2.061×10^{19}	195
D-3803-2	A-0313	2.061×10^{19}	196
D-3803-3	C-1279	2.061×10^{19}	195
D-3804-1	C-1308A	2.061×10^{19}	188
D-3804-2	C-1308B	2.061×10^{19}	161
D-3804-3	B-5294	2.061×10^{19}	107

*circumferential weld subject to 300°F limit

Reply to Request for Additional Information Regarding Reactor Pressure Vessel Neutron Fluence Evaluation

NRC Question 16a

Regarding page 6 of Attachment 1 of your letter of February 21, 2000, how was the ultrasonic flow measurement (UFM) used to determine the 2% underpower operation?

Response to Question 16a

The feedwater flow measurement with and without the UFM was utilized as an input parameter into the heat balance equation of the plant. By comparing the thermal energy of the core using the feedwater flow as measured by the venturis and the UFM, it was determined that the core thermal power on average was 2% lower than rated hot full power conditions from Cycle 1 through 12 due to an error in the calibration of one of the venturis, and a phenomena called 'venturi fouling.' See Section 16.4 below for a detailed discussion.

NRC Question 16b

What error, if any, is associated with the UFM?

Response to Question 16b

The 95% confidence interval for the UFM corrected flow measurements has been calculated to be 0.51%. This error is smaller than the error associated with the venturi measured feedwater flow (0.99%) which is utilized in the heat balance equation. See Section 16.3 below for a detailed discussion of the calculation of the error associated with the UFM corrected flow measurement.

NRC Question 16c

What data demonstrate the UFM correction?

Response to Question 16c

Data from the Palisades Procedure DWT-8 "UFM Data Collection, Analysis, And Implementation" has been collected on a biweekly basis since the middle of Cycle 13 (September 1997). On average, the correction factor has been 2.39% with a 95% confidence interval of ±0.089%. See Section 16.4 below for a demonstration of the collected UFM mass flow rate data and the associated increase in thermal power.

Reply to Request for Additional Information Regarding Reactor Pressure Vessel Neutron Fluence Evaluation

16.1 INTRODUCTION

Palisades uses the flow indicated by two feedwater flow venturis (one on each feedwater loop) as input parameters to the heat balance power calculation. The heat balance power calculation is the main (and most accurate) method available at the plant to determine the actual reactor thermal power and to verify that Hot Full Power (HFP) license limits are not exceeded. Accurate measurements of the feedwater flow are required to adequately determine reactor power.

The two feedwater flow venturis were calibrated prior to operation of the plant in Cycle 1. During the beginning of Cycle 1 a flow straightener detached from one of the feedwater flow lines and slammed into its flow venturi. The damaged venturi was removed, repaired, and calibrated offsite prior to reinstallation at the plant. Both flow straighteners were removed from the two feedwater lines to prevent a similar occurrence.

The undamaged flow venturi was not recalibrated following the removal of its flow straightener. The plant operated in this condition until mid-Cycle 13 when an Ultrasonic Flow Measurement (UFM) system was placed in service. Extensive feedwater flow measurements were conducted using the highly accurate UFMs. These flow measurements were used as input parameters to the heat balance calculation and revealed that the reactor was operating, on average, more than 2% below HFP license limits.

Adjustments to the fluence estimates which account for the "UFM-Correction" for plant operation at less than the rated power level during Cycles 1-12, are determined by reducing the cycle lengths (EFPDs) by 2%. It was conservatively chosen to make no correction for the early portion of Cycle 13 when the UFM was not yet in service. The "UFM Correction" for historical operating data is not applicable to the estimated fluence for the latter portion of Cycle 13 and later cycles after the UFM was placed in service.

16.2 METHODOLOGY FOR DETERMINING THE UFM-CORRECTED POWER LEVEL

The plant operated with the conservatively biased venturi calibration until mid-Cycle 13 when an Ultrasonic Flow Measurement (UFM) system was placed in service. Extensive feedwater flow measurements were conducted using the highly accurate UFMs. These flow measurements were used as input parameters to the heat balance calculation and revealed that the reactor was operating, on average more than 2% below HFP license limits.

The heat balance equation is simply a energy balance between the primary and secondary system of the plant:

$$Q_{Rx} = [Q_{SG} + Q_{LD} + Q_{FL}] - [Q_{PCP} + Q_{PZR} + Q_{CH}]$$

where,

Q_{Rx} = Heat Produced by the Reactor
Q_{SG} = Heat Removed by Steam Generators
Q_{LD} = Heat Removed by Letdown Flow
Q_{FL} = Heat Removed by Fixed Insulation Losses
Q_{PCP} = Heat Produced by Primary Coolant Pumps
Q_{PZR} = Heat Produced by the Pressurizer
Q_{CH} = Heat Produced by the Charging System

During steady state full power operations, the heat removed from the primary system to the steam generators, Q_{SG}, amounts to more than 99% of the total heat balance. During steady state, it is assumed that the feedwater mass flow rate equals the mass flowrate in the steam lines. Therefore, the main contributor to the error in the heat balance equation will be the errors associated with the measurements of the feedwater mass flow rates. The accurate readings of the UFM feedwater flow measurement improve the capability of accurately estimating the amount of heat generated in the core compared to the venturi measurements.

16.3 ERROR ASSOCIATED WITH THE UFM MEASUREMENT DATA

16.3.1 Methodology

The determination of the statistical uncertainty presented in this section follows the guidelines provided in ANSI standard ANSI/ISA-S67.04-Part I-1994, "Setpoints for Nuclear Safety Related Instrumentation", and ISA-RP67.04-Part II-1994, "Methodologies for the Determination of Setpoints for Nuclear Safety Related Instrumentation." The appropriate uncertainty terms are combined statistically to determine an uncertainty for the correction factor X = (Average UFM Flow/ Average Venturi Flow). Correction factor and venturi uncertainty are then combined to yield an uncertainty in the UFM corrected feedwater flow measurement.

The following relationship describes the UFM corrected feedwater flow measurement:

$$FW = X * V$$

where,

$$X = \frac{\text{Average UFM Feedwater Flow}}{\text{Average Venturi Feedwater Flow}}$$

FW = Average UFM Feedwater Flow

V = Plant Computer venturi based feedwater flow reading

Using the Square Root of Sum of Square errors (SRSS) method to determine the uncertainty in feedwater flow as a function of the uncertainty in the UFM correction factor and the uncertainty in the venturi flow uncertainties yields:

$$\varepsilon^2_{FW} = [\varepsilon^2_X + \varepsilon^2_V]$$

where, ε = 95% confidence interval.

16.3.2 Venturi Uncertainty Components

The empirical flow uncertainty for the venturi measurement loop at full power is given by:

$$FE_{ERROR} + AS\ LEFT_{ERROR} \pm PPC(SQRT_{ERROR} \text{ and } (TE)\ FLOW_{ERROR}) =$$

$$= 0.5\% + 0.25\% \pm 0.24\% = 0.99\%$$

Where FE_{ERROR} is the factory calibration error of the venturi itself (0.5% is the worst of the two), AS $LEFT_{ERROR}$ is the worst loop calibration error and PPC is a combination of temperature element errors and the error introduced by a transfer function of a nonlinear module. The UFM is implemented as an independent calibration of the venturi loop. It is therefore inappropriate to consider FE_{ERROR} and AS $LEFT_{ERROR}$ in the UFM corrected feedwater flow error analysis. The contribution to the uncertainty due to the PPC venturi flow measurement is given by:

$$\varepsilon^2_V = [PPC(SQRT_{ERROR} \text{ and } (TE)FLOW_{ERROR})]^2$$

$$\varepsilon^2_V = (0.24)^2 = 0.0576$$

where,

ε = 95% confidence interval
V = Venturi flow measurement

16.3.3 UFM Correction Factor Uncertainty

The UFM correction factor to feedwater flow is given by

$$X = \frac{\text{Average UFM Feedwater Flow}}{\text{Average Venturi Feedwater Flow}}$$

The uncertainty of X is determined using the following relationship:

$$\varepsilon^2_X = [\varepsilon^2_w + \varepsilon^2_{Va}]$$

where,

ε = 95% confidence interval
X = the UFM correction factor
w = UFM feedwater flow measurement
Va = average venturi flow measurement

16.3.4 UFM Uncertainty Components

The 95% confidence interval of the feedwater UFM is given by:

$$\varepsilon^2_w = [\varepsilon^2_{Cf} + \varepsilon^2_A + \varepsilon^2_L + \varepsilon^2_{\Delta t} + \varepsilon^2_\rho]$$

where,

ε = 95% confidence interval
w = UFM feedwater flow measurement
C_f = the flow profile correction factor
ρ= the density of the feedwater
A = the cross-sectional area of the feed water pipe
L = the spacing between the upstream and downstream transducer of the CROSSFLOW meter
Δt = the residence time of the eddies within the flow; the time it takes to pass between the two sets of transducers.

In a letter to Consumers Energy dated July 1997, ABB specifies the uncertainty components in the above equation. These uncertainties are specified for each of the two flow loops at Palisades. This uncertainty analysis was performed by ABB. The analysis assumes the largest reported value for each of the above uncertainties including a value of $\varepsilon_{\Delta t}$ corresponding to 60 data points with a relative standard deviation of less than 0.60%. Although the electronics in the UFM setup are not expected to drift, ABB has included a system electronics uncertainty component that is associated with drift. A calculation using a test signal is routinely performed and verifies that the system responds properly. This check would identify any signs of drift in the measured values. This test is performed periodically as part of the Palisades procedure DWT-08 "UFM Data Collection, Analysis, And Implementation." The uncertainty developed in this section includes the electronics uncertainty as specified by ABB.

It is also reasonable to expect an uncertainty associated with the physical placement of the transducers on the feedwater piping. It is the intention not to move the transducers from the locations evaluated by ABB. Errors associated with possible small movements due to vibration or expansion have not been evaluated. These errors are believed to be small compared to the others considered, and are therefore ignored in this analysis.

Incorporating values for the above uncertainties, the 95% confidence interval for the UFM feedwater flow measurements becomes:

$$\varepsilon^2_w = [\varepsilon^2_{Cf} + \varepsilon^2_A + \varepsilon^2_L + \varepsilon^2_{\Delta t} + \varepsilon^2_\rho]$$

$$\varepsilon^2_w = [(0.2745)^2 + (2 \times 0.0898)^2 + (0.0967)^2 + (0.2296)^2 + (0.1670)^2]$$

$$\varepsilon^2_w = 0.1976$$

$$\varepsilon_w = 0.4445\%$$

16.3.5 Average Venturi Flow Uncertainty

The venturi flow uncertainty is given in Section 16.3.2. The uncertainty of the average can be determined from Palisades procedure DWT-8 as follows:

$$\varepsilon_{Va} = \frac{\varepsilon_v}{\sqrt{n}}$$

where,

ε = 95% confidence interval
Va = average venturi flow measurement
V = venturi flow measurement
N = number of venturi flow measurements considered in average

The number of points included in each hour average is determined in the Plant Process Computer (PPC). The PPC updates the feedwater flow once per second. A rolling average of these one second snapshots is used to filter the values. The hour averages are composed of ten minute averages which are composed of snapshots taken at a one minute interval. Each level requires that 90% of the points being averaged are valid. Therefore, if we conservatively ignore the filtering taking place for each second update, the minimum number of points which could make up a valid hour average venturi feedwater flow is 45. Taking the value of ε_V from Section 16.3.2, the uncertainty in the three-hour rolling average venturi flow measurement becomes:

$$\varepsilon_{Va} = \frac{\varepsilon_v}{\sqrt{n}}$$

$$\varepsilon_{Va} = \frac{0.24}{\sqrt{3 * 45}}$$

$$\varepsilon_{Va} = 0.022\%$$

$$\varepsilon^2_{Va} = 4.8 \times 10^{-4}$$

16.3.6 Total UFM Corrected Feedwater Flow Uncertainty

Combination of the terms in the previous sections yields the uncertainty in the UFM corrected feedwater flow:

$$\varepsilon^2_{FW} = [\varepsilon^2_X + \varepsilon^2_V] \text{ and } \varepsilon^2_X = [\varepsilon^2_w + \varepsilon^2_{Va}]$$

which becomes:

$$\varepsilon^2_{FW} = [\varepsilon^2_w + \varepsilon^2_{Va} + \varepsilon^2_V]$$

Utilizing values of the different uncertainty terms derived in this section yields the following result for the total UFM corrected flow uncertainty:

$$\varepsilon^2_{FW} = [0.1976 + 4.8 \times 10^{-4} + 0.0576] = 0.2557$$

and

$$\varepsilon_{FW} = 0.51\%$$

The venturi only uncertainty from Section 16.3.2 (0.99%) bounds the UFM corrected feedwater flow uncertainty (ε_{FW} = 0.51%).

16.4 DATA FOR CYCLE 13 THROUGH 15 DEMONSTRATING THE UFM-CORRECTED POWER LEVEL

A significant source of the difference between the venturi measurements and the UFM is due to 'venturi fouling', or crud buildup on the venturis, the UFM correction factor is only applicable in the condition when it was established. When a plant condition is changed, the UFM correction factor has to be recalculated, based on measured data. For conditions in which the power level is changing, a conservative measurement of the feedwater flow is needed, so that HFP license limits are not exceeded. The venturi measured feedwater flow is known to result in lower thermal output, and it is therefore conservative. During changes in the reactor power levels, a UFM correction factor of 1.0 is utilized (no UFM correction is utilized). Since the UFM flow correction factors are incrementally increased, values below 2% are utilized periodically.

Section 16.2 shows that the result of the heat balance is more accurate using the UFM data than using the measurement data from the feedwater flow venturis (0.51% vs. 0.99%).

Table 16-1 presents the UFM corrections for each loop for mid cycle 13 through present time (beginning of cycle 15). In Table 16-2, it is shown that the UFM correction is on average 2.389%, with a 95% confidence interval of ± 0.0885%. Based on this data, an average UFM correction of 2% was conservatively chosen for Cycles 1 through 12.

Table 16-1: UFM Data for Mid-Cycle 13 through 15

Cycle	Date	Calc A	Calc B	Calc Total
13	09/23/1997	0.9802	0.9627	2.855%
	10/25/1997	0.9850	0.9650	2.500%
	10/30/1997	0.9853	0.9676	2.355%
	11/12/1997	0.9910	0.9679	2.055%
	11/25/1997	0.9868	0.9692	2.200%
	12/10/1997	0.9834	0.9660	2.530%
	12/22/1997	0.9811	0.9647	2.710%
	01/06/1998	0.9804	0.9631	2.825%
	01/21/1998	0.9824	0.9637	2.695%
	02/04/1998	0.9838	0.9637	2.625%
	02/17/1998	0.9862	0.9632	2.530%
	03/04/1998	0.9825	0.9669	2.530%
14	06/17/1998	0.9922	0.9839	1.195%
	06/25/1998	0.9955	0.9628	2.085%
	07/08/1998	0.9853	0.9751	1.980%
	07/31/1998	0.9883	0.9774	1.715%
	08/05/1998	0.9873	0.9664	2.315%
	08/19/1998	0.9832	0.9705	2.315%
	09/02/1998	0.9817	0.9717	2.330%
	09/16/1998	0.9828	0.9751	2.105%
	09/29/1998	0.9862	0.9771	1.835%
	10/14/1998	0.9807	0.9732	2.305%
	10/22/1998	0.9783	0.9690	2.635%
	10/29/1998	0.9811	0.9762	2.135%
	11/11/1998	0.9815	0.9742	2.215%
	11/25/1998	0.9838	0.9733	2.145%
	12/09/1998	0.9852	0.9730	2.090%
	01/17/1999	0.9941	0.9780	1.395%
	01/22/1999	0.9794	0.9653	2.765%
	02/11/1999	0.9837	0.9774	1.945%
	02/17/1999	0.9832	0.9756	2.060%
	03/03/1999	0.9823	0.9739	2.190%
	03/17/1999	0.9817	0.9749	2.170%
	03/22/1999	0.9831	0.9758	2.055%
	03/31/1999	0.9811	0.9776	2.065%
	04/14/1999	0.9804	0.9747	2.245%
	04/21/1999	0.9802	0.9820	1.890%
	04/26/1999	0.9808	0.9739	2.265%
	05/23/1999	0.9812	0.9802	1.930%
	05/26/1999	0.9787	0.9752	2.305%
	06/09/1999	0.9775	0.9754	2.355%
	06/23/1999	0.9756	0.9778	2.330%
	07/07/1999	0.9697	0.9762	2.705%
	07/21/1999	0.9745	0.9757	2.490%
	08/04/1999	0.9730	0.9769	2.505%
	08/18/1999	0.9761	0.9774	2.325%
	09/01/1999	0.9742	0.9776	2.410%
	09/14/1999	0.9784	0.9773	2.215%
	09/29/1999	0.9769	0.9768	2.315%

15	02/02/2000	0.9842	0.9750	2.042%
	03/10/2000	0.9835	0.9770	1.977%
	03/19/2000	0.9829	0.9775	1.980%
	03/27/2000	0.9835	0.9781	1.922%

Table 16-2: Statistical Analysis of the UFM Data for Mid-Cycle 13 through 15

	All Data
Average:	2.239%
STDEV:	0.329%
# Data Points:	53
α:	0.05
95% Confidence Interval:	0.0885%

Reply to Request for Additional Information Regarding Reactor Pressure Vessel Neutron Fluence Evaluation

NRC Question 17

In your letter of February 21, 2000, forwarding WCAP-15353, Revision 0, you request that the NRC staff approve that "the Palisades reactor vessel is not expected to reach the PTS [pressurized thermal shock] screening criteria until 2014." Per the PTS Rule (Title 10 of the Code of Federal Regulations Part 50 Section 61), PTS evaluations are characteristically made and reviewed relative to the expiration date of a facility's operating license (see in particular 10 CFR 50.61(a)(6) on end-of-life fluence). As such, the NRC staff requests that you provide an appropriately detailed evaluation for each Palisades beltline material (citing copper and nickel compositional values, fluence values, margin terms, the relevance of any reactor vessel surveillance data to the assessment, etc.) to demonstrate what their RT_{PTS} values will be at the end of your current operating license. By separate application dated April 27, 2000, you have also requested an amendment to recapture Palisades' period of construction by extending the current operating license by four years (i.e., from March 14, 2007, to March 24, 2011). Therefore, you should also submit an evaluation for each beltline material for the end of the operating license, including the proposed construction period recapture.

Response to Question 17

Material properties (copper and nickel concentrations, margin and $RT_{NDT(u)}$ are taken from the Reactor Vessel Integrity Database, Version 2, which reflects all of our responses to Generic Letter 92-01. Our most recent response[1] included an assessment of available reactor vessel surveillance data. It was concluded in that submittal that the best estimate copper and nickel concentrations of the beltline materials appropriately represent the best estimate chemistry factor (CF) for each material.

[1]Haskell (Consumers) to NRC, "Docket 50-255 - License DPR-20 - Palisades Plant - Response to Request for Additional Information Regarding Reactor Pressure Vessel Integrity (TAC No. MA0560)," September 8, 1998

Reply to Request for Additional Information Regarding Reactor Pressure Vessel Neutron Fluence Evaluation

The projected RT_{PTS} for each of the reactor vessel beltline materials on March 14, 2007 is:

Component Identification	Heat #	Cu%	Ni%	EOL Fluence (n/cm²)	$RT_{NDT(u)}$ (°F)	Margin (°F)	RT_{PTS} (°F)
2-112A/C	W5214	0.213	1.01	1.373×10^{19}	-56	65.5	261
3-112A/C	W5214	0.213	1.01	1.373×10^{19}	-56	65.5	261
	34B009	0.192	0.980	1.373×10^{19}	-56	65.5	246
9-112	27204	0.203	1.018	1.873×10^{19}	-56	65.5	275*
D-3803-1	C-1279	0.24	0.50	1.873×10^{19}	-5	17	192
D-3803-2	A-0313	0.24	0.52	1.873×10^{19}	-30	34	192
D-3803-3	C-1279	0.24	0.50	1.873×10^{19}	-5	17	192
D-3804-1	C-1308A	0.19	0.48	1.873×10^{19}	0	34	185
D-3804-2	C-1308B	0.19	0.50	1.873×10^{19}	-30	34	158
D-3804-3	B-5294	0.12	0.55	1.873×10^{19}	-25	34	105

*circumferential weld subject to 300°F limit

Reply to Request for Additional Information Regarding Reactor Pressure Vessel Neutron Fluence Evaluation

The projected RT_{PTS} for each of the reactor vessel beltline materials on March 24, 2011 is:

Component Identification	Heat #	Cu%	Ni%	EOL Fluence (n/cm²)	$RT_{NDT(u)}$ (°F)	Margin (°F)	RT_{PTS} (°F)
2-112A/C	W5214	0.213	1.01	1.492×10^{19}	-56	65.5	266
3-112A/C	W5214	0.213	1.01	1.492×10^{19}	-56	65.5	266
	34B009	0.192	0.980	1.492×10^{19}	-56	65.5	251
9-112	27204	0.203	1.018	2.061×10^{19}	-56	65.5	281*
D-3803-1	C-1279	0.24	0.50	2.061×10^{19}	-5	17	195
D-3803-2	A-0313	0.24	0.52	2.061×10^{19}	-30	34	196
D-3803-3	C-1279	0.24	0.50	2.061×10^{19}	-5	17	195
D-3804-1	C-1308A	0.19	0.48	2.061×10^{19}	0	34	188
D-3804-2	C-1308B	0.19	0.50	2.061×10^{19}	-30	34	161
D-3804-3	B-5294	0.12	0.55	2.061×10^{19}	-25	34	107

*circumferential weld subject to 300°F limit

ATTACHMENT 2

CONSUMERS ENERGY COMPANY
PALISADES PLANT
DOCKET 50-255

July 6, 2000

Additional Information Regarding Theoretical Adjustment of Reactor Vessel Surveillance Data

28 Pages

Additional Information Regarding Theoretical Adjustment of Reactor Vessel Surveillance Data

NRC Question 9a

On page 3-15, it is stated that FERRET has "...assigned uncertainties and correlations..." What are the values and why are they relevant to this application?

Response to Question 9a

The predicted pressure vessel fluence that was generated in WCAP-15353 for Palisades is based solely on the results of the absolute transport calculations. The least squares adjustment was not used to derive the projected vessel fluence and was only provided for comparison purposes with our prior reports and submittals. In the interest of completeness, however, the following additional information is provided as it relates to the theoretical adjustment of reactor vessel surveillance data.

The SAND-II/FERRET least squares adjustment procedure was utilized to produce a best fit among the calculated neutron spectrum at each sensor set location and the set of measured reaction rates from the multiple foil dosimetry sets irradiated at the Palisades reactor. In this methodology, uncertainties in the derived exposure rates [$\phi(E > 1.0$ MeV), $\phi(E > 0.1$ MeV), and dpa] at the measurement locations are dependent on the resultant fit of the adjusted spectrum to the measured data which includes a combination of the uncertainties in measured reaction rates, sensor cross-sections, and the calculated spectrum. For a more-detailed description of the least squared adjustment procedure, see Section 9.1 of this response below.

The uncertainties that are associated with the measured reaction rates used in the Palisades dosimetry evaluations is as follows:

Reaction	Reaction Rate Uncertainty
$^{63}Cu\ (n,\alpha)\ ^{60}Co$	5%
$^{46}Ti\ (n,p)\ ^{46}Sc$	5%
$^{54}Fe\ (n,p)\ ^{54}Mn$	5%
$^{58}Ni\ (n,p)\ ^{58}Co$	5%
$^{238}U\ (n,f)\ ^{137}Cs$	10%
$^{237}Np\ (n,f)\ ^{137}Cs$	10%
$^{59}Co\ (n,\gamma)\ ^{60}Co$	5%

Additional Information Regarding Theoretical Adjustment of Reactor Vessel Surveillance Data

These uncertainty values are quoted at the 1σ level. The justification/relevance for the aforementioned measured reaction rate uncertainties is discussed in Sections 9.2 and 9.3 of this response.

The dosimetry cross-sections that were utilized in this evaluation were taken directly from the SNLRML evaluated dosimetry cross-section library (DLC-178, RSIC Data Library Collection SNLRML, Recommended Dosimetry Cross Section Compendium, July 1994). The uncertainties that are associated with the SNLRML cross-sections are in the form of variances and covariances that are provided along with the basic dosimetry cross-section data.

For sensors of interest to the Palisades evaluation and Light Water Reactor dosimetry applications in general, the following uncertainties in the fission spectrum averaged cross-sections were provided in DLC-178.

Reaction	Uncertainty
^{63}Cu (n,α) ^{60}Co	4.08-4.16%
^{46}Ti (n,p) ^{46}Sc	4.51-4.87%
^{54}Fe (n,p) ^{54}Mn	3.05-3.11%
^{58}Ni (n,p) ^{58}Co	4.49-4.56%
^{238}U (n,f) ^{137}Cs	0.54-0.64%
^{237}Np (n,f) ^{137}Cs	10.32-10.97%
^{59}Co (n,γ) ^{60}Co	0.79-3.59%

Since the SNLRML library has been empirically tested for use in fission spectra determination as well as in the fluence and energy characterization of 14 MeV neutron sources, its use is relevant to the current Palisades evaluation. Also note that additional material on the dosimetry cross-section uncertainties may be found in Sections 9.2 and 9.4 of this response.

The uncertainties in the calculated neutron energy spectrum at the location of the individual sensor sets are also input in the form of variances and covariances with the following specifications:

Additional Information Regarding Theoretical Adjustment of Reactor Vessel Surveillance Data

Flux Normalization Uncertainty	15%
Flux Group Uncertainties	
(E > 0.0055 MeV)	15%
(0.68 eV < E < 0.0055 MeV)	29%
(E < 0.68 eV)	52%
Short Range Correlation	
(E > 0.0055 MeV)	0.9
(0.68 eV < E < 0.0055 MeV)	0.5
(E < 0.68 eV)	0.5
Flux Group Correlation Range	
(E > 0.0055 MeV)	6
(0.68 eV < E < 0.0055 MeV)	3
(E < 0.68 eV)	2

It should be noted that these uncertainties are relevant to the current Palisades evaluation since they are consistent with the corresponding 14% calculated uncertainty that was documented in WCAP-15353. Furthermore, it is also worthwhile mentioning that per the NRC Staff's request, the aforementioned flux normalization and group uncertainties are a factor of two lower relative to previous analyses that were performed for Palisades (see, for example, WCAP-14557, Revision 1, or the associated NRC RAI Responses dated 07/31/98).

NRC Question 9b

On page 3-18, it is stated that the values are "liberal enough" to fit the measured data for all practical applications. Are these values the product of judgement and selection or the product of some arithmetic or mathematical operation? These uncertainty assignments are stated to be a product of FERRET applications, but page 3-17 appears to indicate that they originated in Maerker's LEPRICON. Please clarify.

Response to NRC Question 9b

The predicted pressure vessel fluence that was generated in WCAP-15353 for Palisades is based solely on the results of the absolute transport calculations. The least squares

adjustment was not used to derive the projected vessel fluence and was only provided for comparison purposes with our prior reports and submittals. In the interest of completeness, however, the following additional information is provided as it relates to the theoretical adjustment of reactor vessel surveillance data.

As indicated in the response to Question 9a above, it is apparent that the FERRET uncertainties have adjusted the input spectrum to fit the measured data quite well since the results are consistent with the 14% calculated uncertainty that was reported for Palisades in WCAP-15353. This has also been typically experienced, in general, for all other dosimetry evaluations that Westinghouse has performed. The large body of previous experience/knowledge, in conjunction with our adherence to national standards and the performance of inter-comparisons with other expert industry groups, has demonstrated that the selected FERRET uncertainties (that are the product of benchmarking and engineering judgement), provide reliable results that are consistent with other well-known organizations. Additional information on the FERRET least squares adjustment procedure, including a detailed discussion of the associated uncertainties, may be found in Sections 9.1 through 9.4 of this response.

With respect to the final portion of Question 9b, the FERRET uncertainties did not originate from LEPRICON. Maerker's work was only used for validation of the uncertainties in FERRET.

9.1 General Discussion

The methodology used in the evaluation of the multiple foil dosimetry sets irradiated at the Palisades reactor utilizes a least squares adjustment procedure to produce a best fit among the calculated neutron spectrum at each sensor set location and the set of measured reaction rates from the dosimetry package. In this methodology, uncertainties in the derived exposure rates [$\phi(E > 1.0$ MeV), $\phi(E > 0.1$ MeV), and dpa] at the measurement locations are dependent on the resultant fit of the adjusted spectrum to the measured data which includes a combination of the uncertainties in measured reaction rates, sensor cross-sections, and the calculated spectrum.

In the analysis performed for the Palisades reactor, both the "best estimate" exposure rates and the associated uncertainties were obtained from the measured reaction rates, dosimetry cross-sections, and the calculated neutron spectra by means of the SAND-II/FERRET least squares adjustment procedure.

The use of an adjustment procedure to evaluate neutron dosimetry from Light Water Reactors is described in ASTM E 944 - 96, "Standard Guide for Application of Neutron

Spectrum Adjustment Methods in Reactor Vessel Surveillance," as follows:

> *"3.3.2.1 The algorithms of the adjustment codes tend to decrease the variances of the adjusted data compared to the corresponding input values. The least squares adjustment codes yield estimates for the output data with minimum variances, that is, the 'best' estimates. This is the primary reason for using these adjustment procedures."*

In using the adjustment procedure, dosimetry measurements are provided as a set of reaction rates denoted by the following symbols:

$$R_i \quad i = 1,2,...$$

Reaction cross-sections for the dosimetry sensors are obtained from the SNLRML ENDF/B-VI based evaluated dosimetry cross-section file. The cross-sections for the ith reaction as a function of energy are denoted by the following:

$$\sigma_i(E) \quad i = 1,2,....$$

The calculated neutron spectrum input to the adjustment procedure are obtained on a location-specific basis from the results of the cycle-specific discrete ordinates transport calculation. The group fluxes from the transport calculation are denoted by the following:

$$\phi_j \quad j = 1,2,...k$$

The uncertainties associated with the measured reaction rates, dosimetry cross-sections, and calculated neutron spectrum are also input to the adjustment procedure in the form of variances and covariances. In the evaluations performed for the Palisades reactor, the assignment of the input uncertainties also follows the guidance provided in the ASTM E 944 standard.

9.2 Uncertainties in the Input to the Adjustment Procedure

<u>Measured Reaction Rates</u>

The determination of the individual reaction rates involves laboratory counting procedures, decay corrections to account for the operating history of the reactor, and corrections for competing reactions within the sensors. Each of these facets of the reaction rate determinations are discussed below.

Additional Information Regarding Theoretical Adjustment of Reactor Vessel Surveillance Data

Counting Procedures

Internal surveillance capsule and ex-vessel reactor cavity dosimetry packages employed at the Palisades reactor consist of comprehensive multiple foil sensor sets that make use of some or all of the following reactions:

$^{63}Cu\ (n,\alpha)\ ^{60}Co$
$^{46}Ti\ (n,p)\ ^{46}Sc$
$^{54}Fe\ (n,p)\ ^{54}Mn$
$^{58}Ni\ (n,p)\ ^{58}Co$
$^{238}U\ (n,f)\ ^{137}Cs$
$^{237}Np\ (n,f)\ ^{137}Cs$
$^{59}Co\ (n,\gamma)\ ^{60}Co$

Following irradiation, the specific activity of each of the irradiated radiometric sensors is determined using the latest version of ASTM counting procedures for each reaction. In particular, the following standards are applicable to the radiometric sensors utilized in LWR programs:

E523 Standard Test Method for Measuring Fast-Neutron Reaction Rates by Radioactivation of Copper

E526 Standard Test Method for Measuring Fast-Neutron Reaction Rates by Radioactivation of Titanium

E263 Standard Test method for Measuring Fast-Neutron Reaction Rates by Radioactivation of Iron

E264 Standard Test Method for Measuring Fast-Neutron Reaction Rates by Radioactivation of Nickel

E704 Standard Test Method for Measuring Reaction Rates by Radioactivation of Uranium-238

E705 Standard Test Method for Measuring Reaction Rates by Radioactivation of Neptunium-237

E481 Standard Test Method for Measuring Neutron Fluence Rate by Radioactivation of Cobalt and Silver

E1005 Standard Method for Application and Analysis of Radiometric Monitors for Reactor Vessel Surveillance

Additional Information Regarding Theoretical Adjustment of Reactor Vessel Surveillance Data

E181 Standard General Methods for Detector Calibration and Analysis of Radionuclides

Following sample preparation and weighing, the activity of each monitor was determined by means of a high resolution gamma spectrometer. In the case of the multiple foil sensor sets, these analyses are performed by direct counting of each of the individual sensors, or, as is sometimes the case with ^{238}U and ^{237}Np fission monitors from internal surveillance capsules, by direct counting preceded by dissolution and chemical separation of cesium from the sensor.

Decay Corrections

Having the measured specific activities, the operating history of the reactor, and the physical characteristics of the sensors, reaction rates referenced to full-power operation are determined from the following equation:

$$R = \frac{A}{N_0 \, F \, Y \sum \frac{P_j}{P_{ref}} \, C_j \, [1 - e^{-\lambda t_j}] \, [e^{-\lambda t_d}]}$$

where,

R	=	Reaction rate averaged over the irradiation period and referenced to operation at a core power level of P_{ref} (rps/nucleus).
A	=	Measured specific activity (dps/gm).
N_0	=	Number of target element atoms per gram of sensor.
F	=	Weight fraction of the target isotope in the sensor material.
Y	=	Number of product atoms produced per reaction.
P_j	=	Average core power level during irradiation period j (MW).
P_{ref}	=	Maximum or reference power level of the reactor (MW).
C_j	=	Calculated ratio of $\phi(E > 1.0 \text{ MeV})$ during irradiation period j to the time weighted average $\phi(E > 1.0 \text{ MeV})$ over the entire irradiation period.
λ	=	Decay constant of the product isotope (1/sec).
t_j	=	Length of irradiation period j (sec).
t_d	=	Decay time following irradiation period j (sec).

and the summation is carried out over the total number of monthly intervals comprising the irradiation period.

Additional Information Regarding Theoretical Adjustment of Reactor Vessel Surveillance Data

In the above equation, the ratio $[P_j]/[P_{ref}]$ accounts for month-by-month variation of power level within any given fuel cycle as well as over multiple fuel cycles. For the sensor sets utilized in surveillance capsule and reactor cavity irradiations, the half-lives of the product isotopes are long enough that a monthly histogram describing reactor operation has proven to be an adequate representation for use in radioactive decay corrections for the reactions of interest in the exposure evaluations. The ratio C_j, calculated for each fuel cycle using discrete ordinates transport technology, accounts for the change in sensor reaction rates caused by variations in flux level induced by changes in core spatial power distributions from fuel cycle to fuel cycle. For a single-cycle irradiation such as is common with cavity dosimetry, C_j is taken to be 1.0. However, for multiple-cycle irradiations, particularly those employing low leakage fuel management, the additional C_j correction must be employed. This additional correction can be quite significant for internal surveillance capsules that have been irradiated for many cycles in a reactor that has transitioned from non-low leakage to low leakage fuel management.

Corrections for Competing Reactions

Prior to using the measured reaction rates in the dosimetry evaluation procedures, additional corrections are made to the ^{238}U measurements to account for the presence of ^{235}U impurities in the sensors as well as to correct for the build-in of plutonium isotopes over the course of the irradiation. These corrections are location and fluence dependent and are derived from the results of the discrete ordinates calculations and, when available, with measurements from paired uranium dosimeters.

In addition to the corrections made for the presence of ^{235}U and the build-in of plutonium isotopes in the ^{238}U fission sensors, corrections are also made to both ^{238}U and ^{237}Np sensors to account for gamma-ray induced fission reactions occurring over the course of the irradiation. These photofission corrections are, likewise, location dependent and are based on the plant specific discrete ordinates transport calculations. For additional information on the photofission correction, refer to the response to question 8a.

Reaction Rate Uncertainties

The overall uncertainty associated with the measured reaction rates used in the evaluation of exposure parameters includes components due to the basic measurement process, the irradiation history corrections, and the corrections for competing reactions in the fission sensors. A matrix of the uncertainties associated with the reactions applicable to the Palisades dosimetry evaluations is as follows:

Additional Information Regarding Theoretical Adjustment of Reactor Vessel Surveillance Data

Reaction	Counting	Decay Correction	Competing Reactions	Net Uncertainty
^{63}Cu (n,) ^{60}Co	3%	2%	0%	4%
^{46}Ti (n,p) ^{46}Sc	3%	4%	0%	5%
^{54}Fe (n,p) ^{54}Mn	3%	2%	0%	4%
^{58}Ni (n,p) ^{58}Co	3%	4%	0%	5%
^{238}U (n,f) ^{137}Cs	5%	3%	4%	7%
^{237}Np (n,f) ^{137}Cs	5%	3%	1%	6%
^{59}Co (n,γ) ^{60}Co	3%	4%	0%	5%

In developing this uncertainty tabulation, the counting component is derived from the expected accuracy using the appropriate ASTM standards. The component due to irradiation history (decay correction term) includes the effects of short versus long product half lives, the product yield in the fission monitors, and target abundance in the sensor material. The uncertainties due to competing reactions were based on the assumption that the error in the calculated correction using the plant specific transport results could be as high as 25%, and the resultant uncertainty in the net reaction rate is then 25% of the total correction. For example, a 25% uncertainty in a 4% photofission correction to a measured dosimeter activity results in a net 1% additional uncertainty in the derived reaction rate.

In addition to the use of the ASTM standards in the evaluation of sensor reaction rates, over the course of the last 18 years these procedures have been tested via round robin counting exercises included as a part of the NRC sponsored Light Water Reactor Surveillance Dosimetry Improvement Program (LWR-SDIP) as well as by evaluation of fluence counting standards provided by the National Institute of Science and Technology (NIST). Each of these counting exercises involved evaluation of neutron sensors typical of those used in light water reactor measurement programs. The results of these studies demonstrated that these procedures do, in fact, produce measured reaction rates within the 1σ uncertainties specified in the above tabulation.

A further consistency check on the measured reaction rates from in-vessel surveillance capsule and reactor cavity dosimetry irradiations is obtained from an examination of the several location and reactor dependent data bases built up over many years of performing reactor dosimetry. Examples of these data bases are provided in WCAP-14044, "Westinghouse Surveillance Capsule Neutron Fluence Re-evaluation," E. P. Lippincott, April 1994. The plant data included in these data bases also lend support to the reaction rate uncertainties specified above.

Additional Information Regarding Theoretical Adjustment of Reactor Vessel Surveillance Data

Dosimetry Cross-Sections

As noted in Section 9.1, the dosimetry cross-sections are taken directly from the SNLRML evaluated dosimetry cross-section data base (DLC-178, RSIC Data Library Collection SNLRML, Recommended Dosimetry Cross Section Compendium, July 1994). Cross-section uncertainties in the form of variances and covariances are provided on this data file along with the basic dosimetry cross-section data.

Calculated Spectrum

The uncertainties in the calculated neutron energy spectrum at the location of the individual sensor sets are also input in the form of variances and covariances with the following specifications:

Flux Normalization Uncertainty	15%
Flux Group Uncertainties	
(E > 0.0055 MeV)	15%
(0.68 eV < E < 0.0055 MeV)	29%
(E < 0.68 eV)	52%
Short Range Correlation	
(E > 0.0055 MeV)	0.9
(0.68 eV < E < 0.0055 MeV)	0.5
(E < 0.68 eV)	0.5
Flux Group Correlation Range	
(E > 0.0055 MeV)	6
(0.68 eV < E < 0.0055 MeV)	3
(E < 0.68 eV)	2

It should be noted that these uncertainties are consistent with the corresponding 14% calculated uncertainty that was documented in WCAP-15353. Finally, it is also worthwhile mentioning that the aforementioned flux normalization and group uncertainties are a factor of two lower relative to previous analyses performed for Palisades (see, for example, WCAP-14557, Revision 1 or the associated NRC RAI Responses dated 07/31/98).

Other Uncertainties

Additional uncertainties such as sensor positioning, vessel inner radius, vessel thickness, and water density variations are evaluated based on sensitivity studies using the transport

code calculations. These additional uncertainties are included after the dosimetry evaluations are completed and are considered an uncertainty in relating the M/C bias factor to positions that are removed from the measurement locations, i.e., the pressure vessel wall.

9.3 Accuracy of Reaction Rate Measurements

The accuracy of the reaction rate measurements obtained from surveillance capsule and reactor cavity irradiations is assured by utilizing laboratory procedures that conform to ASTM National Consensus Standards for each of the sensors comprising the multiple foil dosimetry sets. In particular, the following standards are applied for the reactions of interest.

Reaction	Standard
^{63}Cu (n,α) ^{60}Co	ASTM-E-523
^{46}Ti (n,p) ^{46}Sc	ASTM-E-526
^{54}Fe (n,p) ^{54}Mn	ASTM-E-263
^{58}Ni (n,p) ^{58}Co	ASTM-E-264
^{238}U (n,f) ^{137}Cs	ASTM-E-704
^{237}Np (n,f) ^{137}Cs	ASTM-E-705
^{59}Co (n,γ) ^{60}Co	ASTM-E-481

In all cases, the latest available versions of the applicable standard are used in the dosimetry evaluations.

From these standards, it is noted that the expected uncertainties in the measured disintegration rates can be summarized as follows:

Reaction	Precision	Bias
^{63}Cu (n,α) ^{60}Co	1%	3%
^{46}Ti (n,p) ^{46}Sc	1%	3%
^{54}Fe (n,p) ^{54}Mn	1%	3%
^{58}Ni (n,p) ^{58}Co	1%	3%
^{238}U (n,f) ^{137}Cs	1%	5%

Additional Information Regarding Theoretical Adjustment of Reactor Vessel Surveillance Data

Reaction	Precision	Bias
^{237}Np (n,f) ^{137}Cs	1%	5%
^{59}Co (n,γ) ^{60}Co	1%	5%

These uncertainties include the impacts of sample weighing, detector calibration, geometry source/detector geometry corrections, and product nuclide branching ratios.

In determining reaction rates from the measured specific activities, the following additional uncertainties are incurred:

Reaction	Fission Yield	Product Half-life	Competing Reactions
^{63}Cu (n,α) ^{60}Co		0.02%	
^{46}Ti (n,p) ^{46}Sc		0.2%	
^{54}Fe (n,p) ^{54}Mn		0.2%	
^{58}Ni (n,p) ^{58}Co		0.2%	
^{238}U (n,f) ^{137}Cs	1%	0.1%	4%
^{237}Np (n,f) ^{137}Cs	2%	0.1%	1%
^{59}Co (n,γ) ^{60}Co		0.02%	

After combining all of these uncertainty components, the sensor reaction rates derived from the counting and data evaluation procedures used for surveillance capsule and cavity dosimetry irradiations typically result in the following net uncertainties associated with the data:

Reaction	Reaction Rate Uncertainty
^{63}Cu (n,α) ^{60}Co	5%
^{46}Ti (n,p) ^{46}Sc	5%
^{54}Fe (n,p) ^{54}Mn	5%
^{58}Ni (n,p) ^{58}Co	5%
^{238}U (n,f) ^{137}Cs	10%
^{237}Np (n,f) ^{137}Cs	10%
^{59}Co (n,γ) ^{60}Co	5%

Additional Information Regarding Theoretical Adjustment of Reactor Vessel Surveillance Data

These uncertainty values are quoted at the 1σ level.

In addition to the use of ASTM National Consensus Standards in the evaluation of sensor reaction rates, over the course of the last 20 years, these procedures have been tested via round robin counting exercises included as a part of the NRC sponsored Light Water Reactor Surveillance Dosimetry Improvement Program (LWR-SDIP) as well as by evaluation of fluence counting standards provided by the National Institute of Science and Technology (NIST). In all, the following five separate counting comparisons were conducted between 1980 and 1996.

1980 Round robin counting of foil sets irradiated at the Thermal Shield Back (TSB) and Pressure Vessel Face (PVF) positions of the PCA simulator.

1981 Round robin counting of additional foil sets included in the first metallurgical simulated surveillance capsule also irradiated in the PCA benchmark mockup.

These two counting exercises involved direct comparisons with measurements obtained by the Hanford Engineering Development Laboratory (HEDL). At the time of these irradiations, HEDL was a prime contractor providing measurement services for the PCA benchmark which were cross-calibrated with NIST and the MOL Laboratory in Belgium.

1985 Counting and evaluation of ^{46}Ti(n,p), ^{54}Fe(n,p), and ^{58}Ni(n,p) certified fluence standards supplied by NIST.

Comparisons with fluence standards involve the determination of the reaction rate of each foil, but also of the spectrum averaged cross-section in the NIST ^{235}U irradiation facility. Thus, the comparisons with the certified fluence test both the measurement process and the energy dependent reaction cross-section used by the vendor.

1992 Counting of NIST foils irradiated in a reactor cavity dosimetry experiment at the Trojan reactor.

This exercise involved duplicate counting of a subset of irradiated foils by both Westinghouse and NIST to assure adequate cross-calibration of the laboratories so that data could be confidently mixed in the overall fluence evaluations performed by NIST and ORNL.

Additional Information Regarding Theoretical Adjustment of Reactor Vessel Surveillance Data

1996 Irradiation of a set of foils used in Westinghouse cavity dosimetry irradiations at the Materials Dosimetry Reference Facility (MDRF) and subsequent comparison with certified results provided by NIST.

Results of these five inter-comparisons are summarized as follows:

	Westinghouse / HEDL		Westinghouse / NIST			
Reaction	1980	1981	1985	1992	1996	Average
^{63}Cu (n,α) ^{60}Co	1.041	1.018		0.969		1.009
^{46}Ti (n,p) ^{46}Sc	1.036		1.012	1.030		1.026
^{54}Fe (n,p) ^{54}Mn	1.006	1.008	1.011	1.056		1.020
^{58}Ni (n,p) ^{58}Co	1.006	0.990	1.028	1.029		1.013
^{238}U (n,f) ^{137}Cs	1.014	1.014			1.097	1.042
^{237}Np (n,f) ^{137}Cs	1.006	1.017			1.017	1.013
^{59}Co (n,γ) ^{60}Co	1.017	1.017				1.017

The comparisons shown in the preceding table demonstrate that the procedures used by Westinghouse in the determination of reaction rates from both in-vessel surveillance capsule irradiations and ex-vessel cavity irradiations have produced accurate and stable results over a period spanning the last 20 years. The cross-comparisons with HEDL and NIST support the uncertainties of 5% for non-fission reactions and 10% for fission reactions that are assigned to Westinghouse reaction rate results.

Further, the certified fluence comparisons performed in 1985 and 1996, support not only the radiometric counting capability of the Westinghouse Analytical Services Laboratory (and its successor, Antech), but also demonstrate the accuracy of the ^{46}Ti(n,p), ^{54}Fe(n,p), ^{58}Ni(n,p), ^{238}U(n,f), and ^{237}Np(n,f) energy dependent reaction cross-sections that are used in the dosimetry evaluations.

9.4 Accuracy of Reaction Rate Cross-Sections

The reaction rate cross-sections used in the neutron fluence evaluations were taken from the RSIC DATA LIBRARY COLLECTION DLC-178 "SNLRML Recommended Dosimetry Cross-Section Compendium," July 1994. This data library provides reaction rate cross-sections and associated uncertainties for 66 dosimetry sensors in common use. These cross-sections were drawn from the most recent cross-section evaluations and they have been compared with each other and evaluated with respect to their accuracy and consistency for spectrum unfolding calculations. The library has been empirically tested for use in fission spectra

determination as well as in the fluence and energy characterization of 14 MeV neutron sources.

For sensors of interest to Light Water Reactor (LWR) dosimetry applications, the following uncertainties in the fission spectrum averaged cross-sections were provided in DLC-178.

Reaction	Uncertainty
^{63}Cu (n,α) ^{60}Co	4.08-4.16%
^{46}Ti (n,p) ^{46}Sc	4.51-4.87%
^{54}Fe (n,p) ^{54}Mn	3.05-3.11%
^{58}Ni (n,p) ^{58}Co	4.49-4.56%
^{238}U (n,f) ^{137}Cs	0.54-0.64%
^{237}Np (n,f) ^{137}Cs	10.32-10.97%
^{59}Co (n,γ) ^{60}Co	0.79-3.59%

Detailed discussions of the contents of the SNLRML library along with the evaluation process for each of the sensors is provided in DLC-178.

The data provided in SNLRML coupled with the certified fluence comparisons discussed earlier demonstrate that reaction rates as well as reaction cross-sections used in the Westinghouse neutron fluence evaluations provide adequate accuracy.

Additional Information Regarding Theoretical Adjustment of Reactor Vessel Surveillance Data

NRC Question 10

In Tables 4.2-6 to 4.2-8, 4.2-13 to 4.3-15, etc., the actual location of the foils and chains do not have the symmetry implied by their first quadrant equivalent (FQE). What is the meaning of the average FQE 30°?

Response to Question 10

The predicted pressure vessel fluence that was generated in WCAP-15353 for Palisades is based solely on the results of the absolute transport calculations. The least squares adjustment was not used to derive the projected vessel fluence and was only provided for comparison purposes with our prior reports and submittals. In the interest of completeness, however, the following additional information is provided as it relates to the theoretical adjustment of reactor vessel surveillance data.

One way of explaining the designated first quadrant equivalent (FQE) location that is reported in Tables 4.2-6 through 4.2-8, 4.2-13 through 4.2-15, and 4.2-20 through 4.2-22 of WCAP-15353 is to provide an example. These tables summarize the sensor reaction rates from the long gradient chains that were irradiated in Cycles 8, 9, and 10/11, respectively. For convenience, Table 4.2-6 will be used for demonstration purposes; however, it is noted that an analogous procedure was used to determine the FQE location that is identified in all of the tables that are mentioned above.

Appendix B of WCAP-15353 provides the irradiation history and measured specific activities of the radiometric monitors that were placed in the Palisades reactor cavity during Cycle 8 operation. Of particular interest is the long gradient chain data that is given on pages B-12 through B-17 since the reference (*sic*, actual) azimuth was typed onto each lab report page. The reference azimuthal angle appearing on these pages are at 30°, 90°, 150°, 210°, 260°, and 340°. If we were to superimpose these gradient chain locations onto Figure 2.2-1 of WCAP-15353 that shows the in-vessel surveillance capsule locations on a cross section of the Palisades reactor vessel, the following observations could be made with respect to the DORT model (see Figure 3.1-2 of WCAP-15353, for example).

- The 90° gradient chain location is adjacent to the in-vessel wall surveillance capsule at 80° and to the in-vessel accelerated surveillance capsule at 60°; this best corresponds to the 90° FQE position in the DORT analytical model.

Additional Information Regarding Theoretical Adjustment of Reactor Vessel Surveillance Data

- The 260° gradient chain is adjacent to the in-vessel wall surveillance capsule at 260° and to the in-vessel accelerated surveillance capsule at 240°; this best corresponds to the 80° FQE position in the DORT model.

- The 340° gradient chain is adjacent to the 330° in-vessel thermal capsule assembly; however, there are no in-vessel accelerated or wall surveillance capsules at this gradient chain location. Since this thermal capsule assembly was not included in the DORT model, the 340° gradient chain is best represented by the 20° FQE position.

- The 30°, 150°, and 210° gradient chain locations are in core octants that do not contain any in-vessel surveillance capsules; these all correspond to the 30° FQE position in the DORT model.

A height- and sensor-dependent average of the reaction rate values is also presented in these tables for the 30°, 150°, and 210° gradient chain locations since they all correspond to the same 30° FQE position. These average values are presented to permit comparison of the reaction rates from these three symmetric locations. The average values are not used elsewhere in the analysis.

For example, the 30° FQE position data that is reported in Table 4.2-6 for the ^{54}Fe (n,p) ^{54}Mn reaction rate appears to be more tightly clustered about the average values in comparison to the analogous data that is presented in Table 4.2-8 for the ^{59}Co (n, γ) ^{60}Co reaction rate. However, this is expected since the ^{54}Fe (n,p) reaction responds to E > 1.0 MeV neutrons whereas the ^{59}Co (n, γ) reaction is a non-threshold reaction that is affected by neutrons of all energies.

Finally, it should also be recognized that there are isolated instances where a single height-dependent reaction rate does not appear to be consistent with the corresponding 30° FQE data. One example of this may be found in Table 4.2-7 for the ^{58}Ni (n,p) ^{58}Co reaction, which responds to E > 1.0 MeV neutrons, at 7.5 feet above the core midplane. In this particular case, the reaction rate that is provided for the Reference 150° gradient chain is substantially lower than the other two 30° FQE locations. However, since this anomaly took place at a location that was 2 feet above the active core and occurs very infrequently given the volume of gradient chain data, it does not have any impact on the analysis that was performed.

Additional Information Regarding Theoretical Adjustment of Reactor Vessel Surveillance Data

NRC Question 11a

In Tables 4.3-1 to 4.3-22, the least squares adjusted value is frequently outside the range of measured and calculated values. Please explain why this is acceptable and why it is physically meaningful.

Response to Question 11a

The predicted pressure vessel fluence that was generated in WCAP-15353 for Palisades is based solely on the results of the absolute transport calculations. The least squares adjustment was not used to derive the projected vessel fluence and was only provided for comparison purposes with our prior reports and submittals. In the interest of completeness, however, the following additional information is provided as it relates to the theoretical adjustment of reactor vessel surveillance data.

When several sensor reactions included in the foil set result in overlapping spectral coverage, the inter-relationship among these various reactions produces an impact on the least squares adjusted (LSA) results in addition to that provided by the relationship between the calculated and measured reaction rates for individual sensors. This, in turn, can result in the observation noted in Question 11a. As long as the overall adjustment remains constrained by the component uncertainties, the results are justified and physically meaningful. A detailed explanation, and accompanying example, that demonstrates these concepts is provided below in Section 11.1 of this response.

NRC Question 11b

The values of $^{59}Co(n,\gamma)$ and $^{59}Co(n,\gamma)$ Cd seem to be problematic (here as well as in other WCAPs). Why are these values acceptable and what are the acceptance criteria?

Response to Question 11b

The predicted pressure vessel fluence that was generated in WCAP-15353 for Palisades is based solely on the results of the absolute transport calculations. The least squares adjustment was not used to derive the projected vessel fluence and was only provided for comparison purposes with our prior reports and submittals. In the interest of completeness, however, the following additional information is provided as it relates to the theoretical adjustment of reactor vessel surveillance data adjustment.

Ninety-five percent of the response from both the bare and cadmium covered $^{59}Co(n,\gamma)$ sensors occurs below 0.00015 MeV. This energy range is substantially below the region

of interest for pressure vessel exposure. In addition, the majority of the response range occurs at energies where the uncertainty in the calculations tends to be somewhat larger than the higher energy regions of the neutron spectrum.

In light of the above, and as discussed in greater detail below in Section 11.2 of this response, the $^{59}Co(n,\gamma)$ and $^{59}Co(n,\gamma)Cd$ measurements yield results that are consistent with the calculations. Furthermore, as will be demonstrated in the response to Request 11c, these sensors have an insignificant impact on the results of the least squares evaluation of the neutron flux above 1.0 MeV. Hence, based on these observations, the $^{59}Co(n,,\gamma)$ and $^{59}Co(n,\gamma)Cd$ data was deemed acceptable.

NRC Question 11c

What would be the effect if the $^{59}Co(n,\gamma)$ and $^{59}Co(n,\gamma)$ Cd reactions were eliminated?

Response to Question 11c

The predicted pressure vessel fluence that was generated in WCAP-15353 for Palisades is based solely on the results of the absolute transport calculations. The least squares adjustment was not used to derive the projected vessel fluence and was only provided for comparison purposes with our prior reports and submittals. In the interest of completeness, however, the following additional information is provided as it relates to the theoretical adjustment of reactor vessel surveillance data.

With respect to the impact associated with eliminating the cobalt reactions from the least squares adjusted results at the measurement locations, a test was established for the reactor cavity midplane sensor sets whereby the subject reactions were removed and the adjusted fast neutron flux (E > 1.0 MeV) was monitored. The results indicate an average impact of 0.6% on the adjusted value with a maximum impact of 2% for a single measurement point. The results demonstrate that eliminating the cobalt reactions from the least squares adjustment has an insignificant effect on the adjusted fast neutron flux (E > 1.0 MeV) at the measurement locations. Additional material that describes this test is provided below in Section 11.3 of this response.

11.1 Detailed Explanation of LSA Values Outside of the Range of Measured and Calculated Values

The measured and calculated reaction rates listed in Tables 4.3-1 to 4.3-22 of WCAP-15353 represent the mean values for these quantities. Each of these parameters

has an associated uncertainty that is an integral part of the least squares evaluation. The degree of adjustment in the least squares evaluation is constrained by the uncertainties associated with the measured reaction rates, calculated neutron spectrum, and dosimeter reaction cross-sections rather than solely by the mean values associated with these inputs. The criteria that should be examined are whether the assigned uncertainties are appropriate and whether the adjustments occur within ranges defined by these uncertainties. When several sensor reactions included in the foil set result in overlapping spectral coverage, as is the case for the portion of the neutron spectrum above 1.0 MeV, the inter-relationship among these various reactions produces an impact on the adjustment in addition to that provided by the relationship between the calculated and measured reaction rates for individual sensors. This, in turn, can result in the observation noted in Request 11a. As long as the overall adjustment remains constrained by the component uncertainties, the results are justified and physically meaningful.

Consider, for example, the case of in-vessel surveillance capsule W290-9 that was irradiated during the ninth operating fuel cycle. The contents of the multiple foil sensor set included in the W290-9 capsule are summarized in Table 11.1-1.

Table 11.1-1: Summary of the Multiple Foil Sensor Set Included in Capsule W-290-9

	90% Response Range	
Reaction of Interest	**Lower Energy [MeV]**	**Upper Energy [MeV]**
$^{63}Cu(n,\alpha)^{60}Co$ Cd covered	5.00	12.00
$^{46}Ti(n,p)^{46}Sc$	4.10	10.50
$^{54}Fe(n,p)^{54}Mn$	2.40	8.80
$^{58}Ni(n,p)^{58}Co$ Cd covered	2.20	8.80
$^{238}U(n,f)FP$ Cd covered	1.50	8.10
$^{237}Np(n,f)FP$ Cd covered	0.58	6.80
$^{59}Co(n,\gamma)^{60}Co$	1.00e-08	1.35e-04
$^{59}Co(n,\gamma)^{60}Co$ Cd covered	8.40e-07	1.43e-04

This set of sensors is consistent with Section 2.1.1 of Draft Regulatory Guide DG-1053, "Calculational and Dosimetry Methods for Determining Pressure Vessel Neutron Fluence," which states:

> *"The selected dosimeter set should provide adequate spectrum coverage. A common set of fast neutron integral detectors is listed in Table 2. Taken together with a low-energy detector such as cobalt (to estimate the thermal*

neutron fluence for determining interference from low-energy activations), the set provides satisfactory neutron spectrum coverage for pressure vessel dosimetry."

The spectrum coverage of the sensor set, as determined by the calculated neutron spectrum within the W290-9 capsule, is summarized in Table 11.1-1 as the 90% response range for each sensor. The 90% response range, a common means of characterizing spectral coverage, is defined such that, for the spectrum in question, 90% of the total response of the sensor occurs between the specified energy limits, with 5% of the response occurring above the upper limit and 5% occurring below the lower limit. From the tabulation of the 90% response ranges, it is noted that six of the sensor reactions provide significant overlapping spectral coverage in the energy range above 1.0 MeV. It is further noted that neither the bare nor the cadmium covered $^{59}Co(n,\gamma)^{60}Co$ reactions exhibit significant response above the 1.0 MeV threshold and, therefore, only provide data supporting the evaluation of the lower end of the neutron spectrum.

The results of the least squares evaluation of the W290-9 capsule are summarized in Tables 11.1-2 and 11.1-3. In Table 11.1-2, the measured, calculated, and best estimate sensor reaction rates are provided along with the associated uncertainties. The tabulated uncertainty is given at the 1σ level. In regard to the uncertainties listed in Table 11.1-2, the following should be noted.

1 - The uncertainties in the measured reaction rates were derived from the measurement process and include uncertainty components as described in the response to Request 9 of this RAI.

2 - The uncertainties in the calculated reaction rates include components associated with the calculated neutron spectrum as well as with the dosimetry reaction cross-sections. These uncertainties are likewise described in the response to Request 9 of this RAI.

3 - The uncertainties in the best estimate reaction rates are the result of the least squares evaluation of the W290-9 sensor set.

An examination of the data provided in Table 11.1-2 shows that the best estimate $^{54}Fe(n,p)^{54}Mn$ and $^{58}Ni(n,p)^{58}Co$ Cd reaction rates fall slightly outside the range of the measured and calculated mean values, while the best estimate reaction rates for all of the remaining sensors fall between the measured and calculated mean. In Table 11.1-3, the degree of adjustment of the measured and calculated sensor reaction rates is provided for each foil contained in the dosimeter set. The degree of adjustment is given on both an

absolute and percentage basis. An examination of Table 11.1-3 shows that in no instance did the adjustment of the calculated reaction rate exceed 1σ. In the case of the measured data, the adjustment of the $^{46}Ti(n,p)^{46}Sc$ reaction rate was 1.2σ while the adjustment of the $^{54}Fe(n,p)^{54}Mn$ reaction rate was 1.02σ. The adjustments to all of the remaining measured reaction rates were well below 1σ.

Table 11.1-2: Comparison of Measured, Calculated, and LSA Sensor Reaction Rates for Capsule W290-9

Reaction	Measured Reac. Rate [rps/atom]	1σ [%]	Calculated Reac. Rate [rps/atom]	1σ [%]	LSA Reac. Rate [rps/atom]	1σ [%]
$^{63}Cu(n,\alpha)^{60}Co$ Cd	5.72e-17	5.0	5.09e-17	20.8	5.60e-17	5.1
$^{46}Ti(n,p)^{46}Sc$	9.29e-16	5.0	7.99e-16	20.8	8.73e-16	4.3
$^{54}Fe(n,p)^{54}Mn$	4.32e-15	5.0	4.51e-15	20.6	4.54e-15	3.8
$^{58}Ni(n,p)^{58}Co$ Cd	5.78e-15	5.0	5.87e-15	20.6	5.90e-15	4.1
$^{238}U(n,f)FP$ Cd	1.45e-14	10.0	1.50e-14	20.2	1.47e-14	4.2
$^{237}Np(n,f)FP$ Cd	6.29e-14	10.0	6.86e-14	21.6	6.40e-14	9.2
$^{59}Co(n,\gamma)^{60}Co$	1.70e-12	5.0	1.48e-12	38.7	1.69e-12	5.1
$^{59}Co(n,\gamma)^{60}Co$ Cd	2.38e-13	5.0	3.12e-13	28.0	2.41e-13	5.0

Table 11.1-3: Summary of Adjustment to Measured and Calculated Sensor Reaction Rates for Capsule W290-9

Reaction	(LSA-M) / M		(LSA-C) / C	
	Absolute	Percent	Absolute	Percent
$^{63}Cu(n,\alpha)^{60}Co$ Cd	-0.021	-2.1	0.100	10.0
$^{46}Ti(n,p)^{46}Sc$	-0.060	-6.0	0.093	9.3
$^{54}Fe(n,p)^{54}Mn$	0.051	5.1	0.006	0.6
$^{58}Ni(n,p)^{58}Co$ Cd	0.022	2.2	0.006	-2.3
$^{238}U(n,f)FP$ Cd	0.015	1.5	-0.023	-6.7
$^{237}Np(n,f)FP$ Cd	0.018	1.8	-0.067	14.4
$^{59}Co(n,\gamma)^{60}Co$	-0.004	-0.4	0.144	-22.7
$^{59}Co(n,\gamma)^{60}Co$ Cd	0.012	1.2	-0.045	-4.5

Based on the comparisons shown in Tables 11.1-2 and 11.1-3, the least squares evaluation of the W290-9 sensor set was constrained well within the uncertainties associated with the measured reaction rates, calculated neutron spectrum, and dosimetry reaction cross-sections. The results of the least squares evaluation of this data set are acceptable and provide physically reasonable best estimates of the sensor reaction rates.

Additional Information Regarding Theoretical Adjustment of Reactor Vessel Surveillance Data

The example provided for Capsule W290-9, is typical of the other sensor sets irradiated at the Palisades plant. In no instance did the least squares evaluations result in adjustments that were outside the constraints established by the uncertainties associated with the input parameters. Thus, the least squares evaluations of these data sets were judged to be acceptable.

11.2 Discussion of Bare and Cadmium Covered $^{59}Co(n,\gamma)$ Reaction Rates

From Table 11.1-1, it can be seen that 95% of the response of both the bare and cadmium covered $^{59}Co(n,\gamma)$ sensors occurs below 0.00015 MeV, an energy range well below the region of interest for pressure vessel exposure. Further, the majority of the response range occurs at energies where the uncertainty in the calculations tends to be somewhat larger than is the case for the higher energy regions of the neutron spectrum. In fact, some analysts would chose to terminate transport calculations at an energy well above the response range of the cobalt sensors, for example, at 0.1 MeV.

A summary of the M/C ratios for both the bare and Cd covered $^{59}Co(n,\gamma)$ sensors irradiated on the midplane of the reactor cavity is given in Table 11.2-1. From this comparison, it is noted that the behavior of the measurements is very consistent relative to the calculations with the bare reaction exhibiting an average M/C ratio of 1.14 with a standard deviation of 7.3% and the Cd covered reaction showing an average M/C ratio of 1.28 with a standard deviation of 4.2%. The variations seen in the observed M/C ratios are consistent with the expected uncertainties in the measured reaction rates. This behavior shows a systematic under-prediction of the low energy neutron flux in the reactor cavity. As will be demonstrated in the response to Request 11.3, this has an insignificant effect on the results of the least squares evaluation of the neutron flux above 1.0 MeV.

Additional Information Regarding Theoretical Adjustment of Reactor Vessel Surveillance Data

Table 11.2-1: Summary of M/C Ratios for the Bare and Cd Covered $^{59}Co(n,\gamma)$ Sensor Reaction Rates on the Reactor Cavity Midplane

Azimuthal Angle (Degrees)	Irradiation Cycle	M/C Bare $^{59}Co(n,\gamma)$	M/C Cd Covered $^{59}Co(n,\gamma)$
74	8	1.13	1.26
64	8	1.08	1.27
39	8	1.24	1.29
84	8/9	1.15	1.23
74	9	1.10	1.24
64	9	1.01	1.23
39	9	1.15	1.25
84	10/11	1.16	1.27
74	10/11	1.11	1.26
64	10/11	1.06	1.25
54	10/11	1.06	1.30
39	10/11	1.24	1.36
24	10/11	1.30	1.41
Average		**1.14**	**1.28**
% Standard Deviation		**7.3**	**4.2**

11.3 Impact of Removing the $^{59}Co(n,\gamma)$ Reaction Rates

Since the prediction of the Palisades reactor vessel fluence was based solely on the results of the absolute transport calculations and comparisons with measurement were not used to modify the calculations in any way, the elimination of the bare and Cd covered cobalt reactions from the evaluation will have no impact on the predicted vessel exposure.

In terms of the least squares adjusted results at the measurement locations, the effect on the adjusted fast neutron flux (E > 1.0 MeV) of eliminating the cobalt reactions from the adjustment procedure was tested for the reactor cavity midplane sensor sets. The results of this test are provided in Table 11.3-1. The data listed in Table 11.3-1 demonstrate that the elimination of the cobalt reactions from the least squares adjustment has an insignificant impact on the adjusted neutron flux (E > 1.0 MeV) at the measurement locations. The data indicate an average impact of 0.6% on the adjusted value with a maximum impact of 2% for a single measurement point. Given the response range of these sensors the results of this comparison are well within expectation.

Additional Information Regarding Theoretical Adjustment of Reactor Vessel Surveillance Data

Table 11.3-1: Comparison of Least Squares Adjusted $\phi(E > 1.0\ MeV)$ With and Without $^{59}Co(n,\gamma)$ Sensor Reaction Rates

		LSA $\phi(E > 1.0\ MeV)$ $(n/cm^2\text{-}s)$		
Azimuthal Angle (Degrees)	**Irradiation Cycle**	**With $^{59}Co(n,\gamma)$ Sensors**	**Without $^{59}Co(n,\gamma)$ Sensors**	**Ratio Without/With**
84	**8/9**	9.33e+08	9.40e+08	1.008
84	**10/11**	6.30e+08	6.35e+08	1.007
74	**8**	1.30e+09	1.31e+09	1.007
74	**9**	8.53e+08	8.61e+08	1.010
74	**10/11**	6.43e+08	6.51e+08	1.013
64	**8**	9.78e+08	9.85e+08	1.007
64	**9**	7.58e+08	7.73e+08	1.020
64	**10/11**	5.95e+08	6.00e+08	1.008
54	**10/11**	4.89e+08	4.90e+08	1.001
39	**8**	6.86e+08	6.87e+08	1.001
39	**9**	4.92e+08	4.93e+08	1.002
39	**10/11**	4.68e+08	4.67e+08	0.999
24	**10/11**	5.47e+08	5.45e+08	0.997
Average				1.006
% Stand. Dev.				0.6

Additional Information Regarding Theoretical Adjustment of Reactor Vessel Surveillance Data

NRC Question 13

The "M/C" values in Tables 4.3-1 to 4.3-22 give a direct comparison of the measured and calculated sensor reaction rates. What was the statistical basis for accepting or rejecting measurements for inclusion in the least squares adjustment procedure?

Response to Question 13

The predicted pressure vessel fluence that was generated in WCAP-15353 for Palisades is based solely on the results of the absolute transport calculations. The least squares adjustment was not used to derive the projected vessel fluence and was only provided for comparison purposes with our prior reports and submittals. In the interest of completeness, however, the following additional information is provided as it relates to the theoretical adjustment of reactor vessel surveillance data.

The overall uncertainty associated with the measured reaction rates includes components due to the basic measurement process, the irradiation history corrections, and the corrections for competing reactions. A high level of accuracy in the reaction rate determinations is assured by utilizing laboratory procedures that conform to the ASTM National Consensus Standards. In all cases, the latest available versions of the applicable standard are used in the dosimetry evaluations.

From these standards, it is noted that the achievable uncertainties in the measured specific activities of each of the sensors comprising typical multiple foil sensor sets are as follows:

Reaction	Precision	Bias
$^{63}Cu(n,\alpha)^{60}Co$	1%	3%
$^{46}Ti(n,p)^{46}Sc$	1%	3%
$^{54}Fe(n,p)^{54}Mn$	1%	3%
$^{58}Ni(n,p)^{58}Co$	1%	3%
$^{238}U(n,f)FP$	1%	5%
$^{237}Np(n,f)FP$	1%	5%
$^{59}Co(n,\gamma)^{60}Co$	1%	5%

These uncertainties include the impacts of counting statistics, sample weighing, detector calibration, source/detector geometry corrections, and product nuclide branching ratios.

Additional Information Regarding Theoretical Adjustment of Reactor Vessel Surveillance Data

In determining reaction rates from the measured specific activities, the following additional uncertainties are incurred:

Reaction	Fission Yield	Product Half-Life	Competing Reactions
$^{63}Cu(n,\alpha)^{60}Co$		0.02%	
$^{46}Ti(n,p)^{46}Sc$		0.2%	
$^{54}Fe(n,p)^{54}Mn$		0.2%	
$^{58}Ni(n,p)^{58}Co$		0.2%	
$^{238}U(n,f)FP$	1%	0.1%	4%
$^{237}Np(n,f)FP$	2%	0.1%	1%
$^{59}Co(n,\gamma)^{60}Co$		0.02%	

After combining all of these uncertainty components, the sensor reaction rates derived from the counting and data evaluation procedures typically result in the following net uncertainties associated with the sensor reaction rates that are input to the least squares evaluation:

Reaction	Reaction Rate Uncertainty
$^{63}Cu(n,\alpha)^{60}Co$	5%
$^{46}Ti(n,p)^{46}Sc$	5%
$^{54}Fe(n,p)^{54}Mn$	5%
$^{58}Ni(n,p)^{58}Co$	5%
$^{238}U(n,f)FP$	10%
$^{237}Np(n,f)FP$	10%
$^{59}Co(n,\gamma)^{60}Co$	5%

In the evaluation of individual dosimetry sets, an additional test on the measured reaction rates is performed using the concept of a measured spectral index. When a series of measurements have been obtained at locations where the relative neutron energy spectrum remains relatively constant (i.e., for a series of repeat measurements at a given geometric location), the ratio of two reaction rates is equivalent to the ratio of their respective spectrum averaged cross-sections. The variation of these observed ratios should be consistent with the uncertainties in the reaction rates themselves. Significant deviations (3σ) from the nominal ratio observed at a given location are grounds for rejection of the measurement.

Additional Information Regarding Theoretical Adjustment of Reactor Vessel Surveillance Data

An additional reason for rejection of measured data is an observation of obvious physical damage to the sensor. For example, in some cases for in-vessel capsules, ^{238}U foils have been observed to decompose and combine with the cadmium thermal neutron shield. In those instances, an accurate measurement of the activity of the sensor, as well as of the weight of the target material, is extremely difficult. Thus, data from these damaged sensors would not be included in the evaluations.